



# Void-Free Layered Polymeric Architectures via Capillary-Action of Nanoporous Films

Jeonyoon Lee, Seth S. Kessler, and Brian L. Wardle\*

Here, a nanomaterial with morphology-controlled nanoscale capillaries is utilized to overcome manufacturing challenges in layered polymeric architectures. It is demonstrated that the capillary pressure from a nanoporous film replaces the need for applied pressure to manufacture void-free layered polymeric architectures. Manufacturing of aerospace-grade advanced carbon fiber composites is performed for the first time without utilizing pressure from an autoclave. Combined with a conductive curing approach, this work allows advanced composites to be manufactured without costly oven or pressure vessel infrastructure. The nanomaterial-enabled capillary pressure is quantified as 50% greater than typical pressures used in such processing, and is anticipated to overcome the limitations imposed by the requirement of high applied pressure in many other applications such as adhesive joining of various bulk materials including metals, press forming, and closed-mold infusion processing of layered composites and polymers.

aligned or woven microfibers.<sup>[7–9]</sup> We show here that, rather than hindering manufacturing, the high surface-to-volume ratio of aligned nanostructures (here, carbon nanotubes, CNTs) assists in manufacturing polymeric layered architectures via strong capillary forces. If nanomaterials are predistributed in a nanoporous network (NPN) with textured morphology, a strong capillary flow of polymer into the nanoscale aligned capillaries of the porous network may be used to assist manufacturing of various polymeric layered architectures, such as aerospace-grade advanced composites studied herein.

Advanced fiber reinforced polymer (FRP) composite materials, comprising microfiber (commonly carbon and glass) reinforced thermoset and thermoplastic matrices, have been widely used in industries such as aerospace, marine, and wind energy where high mass-specific structural performance is required. Manufacturing of those materials has traditionally focused on layered polymeric architectures processed by an autoclave or other pressure-controlled process to achieve high fiber volume fractions and low void content, resulting in high-quality reproducible parts.<sup>[10,11]</sup> In particular, autoclave processing techniques are primarily performed with prepregs—in which reinforcement fibers are preimpregnated with a polymer matrix material to form a layer—due to their easiness of use, resulting quality, and exceptional mechanical performance. Conventional autoclave-formulated prepreg (hereafter “autoclave prepreg”) is intended to be cured in a vacuum bag ( $\approx 0.1$  MPa) with an applied pressure of 0.6–0.7 MPa to suppress the formation and growth of voids.<sup>[10,12–14]</sup> Without an applied pressure, the composite laminate shows significant amounts ( $\approx 5$  vol%) of voids (see Section S1 in the Supporting Information for the results of curing autoclave prepreg laminates without an applied pressure). An applied pressure is required because voids within a composite laminate cause detrimental effects to structural performance and lifespan of composite parts.<sup>[15–20]</sup> In particular, matrix-dominated properties such as interlaminar shear strength, flexural strength, and fatigue resistance are significantly degraded by the existence of voids, especially due to voids at the interface or the composite layers, known as the interlaminar regions.<sup>[10,21]</sup> Thus, reducing void content has been a focus in the manufacturing of these materials. Manufacturing composites within an autoclave is also accompanied by high acquisition and operating costs of the autoclave infrastructure because a specialized heated vessel using high

## 1. Introduction

In heterogeneous materials, such as fiber-reinforced composites, the increasing focus on nanoscale versus microscale reinforcement architectures offers several advantages in physical properties due to the larger surface area, and therefore interfacial area, for a given volume.<sup>[1,2]</sup> The interfacial area and its properties can dominate the chemical and physical interactions when multiphase materials are formed.<sup>[3]</sup> While the properties of a nanostructured material are mostly influenced by the scale of its constituents and properties of the network they form,<sup>[2]</sup> dispersion of nanomaterials in polymeric materials is broadly problematic in manufacturing of multiphase materials such as polymer nanocomposites.<sup>[4–6]</sup> A homogeneous dispersion of nanomaterials in polymeric materials by using existing compounding techniques is challenging due to the strong tendency of nanomaterials to agglomerate, and is incompatible with many forming technologies that requires combining with

tries such as aerospace, marine, and wind energy where high mass-specific structural performance is required. Manufacturing of those materials has traditionally focused on layered polymeric architectures processed by an autoclave or other pressure-controlled process to achieve high fiber volume fractions and low void content, resulting in high-quality reproducible parts.<sup>[10,11]</sup> In particular, autoclave processing techniques are primarily performed with prepregs—in which reinforcement fibers are preimpregnated with a polymer matrix material to form a layer—due to their easiness of use, resulting quality, and exceptional mechanical performance. Conventional autoclave-formulated prepreg (hereafter “autoclave prepreg”) is intended to be cured in a vacuum bag ( $\approx 0.1$  MPa) with an applied pressure of 0.6–0.7 MPa to suppress the formation and growth of voids.<sup>[10,12–14]</sup> Without an applied pressure, the composite laminate shows significant amounts ( $\approx 5$  vol%) of voids (see Section S1 in the Supporting Information for the results of curing autoclave prepreg laminates without an applied pressure). An applied pressure is required because voids within a composite laminate cause detrimental effects to structural performance and lifespan of composite parts.<sup>[15–20]</sup> In particular, matrix-dominated properties such as interlaminar shear strength, flexural strength, and fatigue resistance are significantly degraded by the existence of voids, especially due to voids at the interface or the composite layers, known as the interlaminar regions.<sup>[10,21]</sup> Thus, reducing void content has been a focus in the manufacturing of these materials. Manufacturing composites within an autoclave is also accompanied by high acquisition and operating costs of the autoclave infrastructure because a specialized heated vessel using high

Dr. J. Lee, Prof. B. L. Wardle  
Department of Aeronautics and Astronautics  
Massachusetts Institute of Technology  
Cambridge, MA 02139, USA  
E-mail: wardle@mit.edu

Dr. S. S. Kessler  
Metis Design Corporation  
Boston, MA 02114, USA

 The ORCID identification number(s) for the author(s) of this article can be found under <https://doi.org/10.1002/admi.201901427>.

DOI: 10.1002/admi.201901427

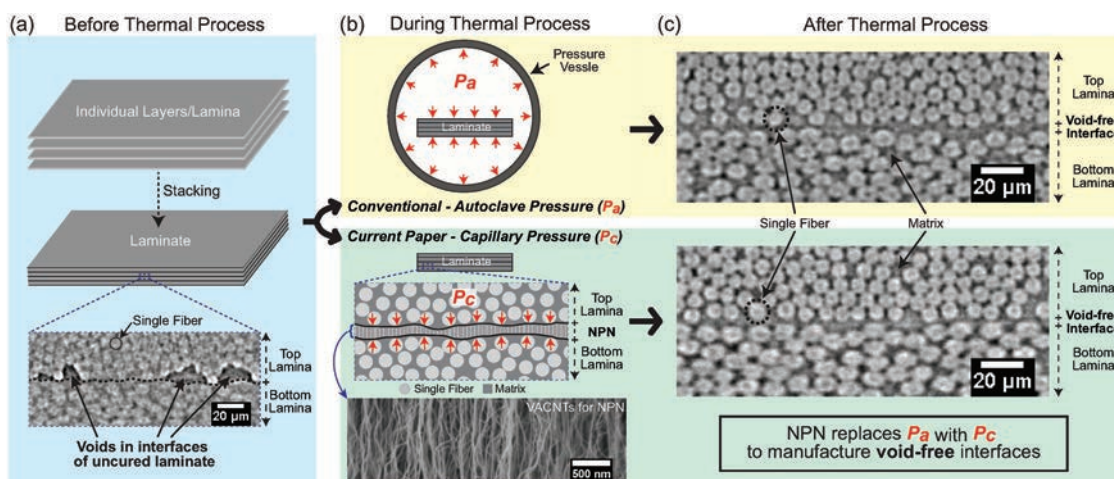


**Figure 1.** Capillary pressure from a nanoporous network (NPN) replaces applied pressure to manufacture void-free polymeric multilayer advanced composites. a) Before thermal processing, uncured laminates have voids at lamina interfaces, as shown in the  $\mu$ CT cross-sectional image. b) During the thermal processing, conventionally, layered polymer composites are processed with applied pressure ( $P_a$ ) from a pressure vessel (autoclave) to suppress voids. Voids can also be removed by utilizing capillary pressure ( $P_c$ ) from NPN comprising VACNTs, which is inserted into the interlaminar regions. In both approaches, vacuum and heat are applied to the laminate as part of the thermal processing; neither is shown. c) After the thermal processing, the voids in the interfaces are removed in both approaches, as presented in the  $\mu$ CT cross-sectional images.

pressures and temperatures is necessary to prevent the formation of voids. Moreover, the size and design of components are constrained by the capacity of autoclaves, and autoclave availability limits the production rate. As such, the interest in the development of alternative techniques has been increased (e.g., induction heating, laser heating, microwave heating, and specially formulated and designed prepregs that can be cured without a pressure vessel—the so-called out-of-autoclave (OoA) prepregs).<sup>[22–24]</sup>

Contrary to autoclave prepregs, pressure vessels are not required for OoA prepregs to achieve a void-free laminate due to the unique morphology/structure of OoA prepregs; e.g., dry regions between resin-rich regions in OoA prepregs function as built-in void extraction channels.<sup>[24–31]</sup> Thus, OoA prepregs can be cured with an oven without an applied pressure, thereby enabling lower cost manufacturing, compared to using autoclave prepregs.<sup>[32,33]</sup> Nevertheless, OoA prepregs are accompanied by modification of resin chemistry to prevent gas emission (“off-gassing”) during curing<sup>[34,35]</sup> and alteration of prepreg morphology for engineering the void extraction channels.<sup>[24]</sup> Hence, these changes require additional processes while manufacturing prepregs. In addition, relatively few prepreg systems are available and even fewer are currently qualified for structural use. Therefore, structural design can be limited due to limited ranges of mechanical properties. Moreover, in contrast to autoclave prepregs, a room-temperature debulking process ranging from a few hours to tens of hours is required for OoA prepregs prior to cure to evacuate entrapped air within a laminate,<sup>[28,29,36,37]</sup> extending the manufacturing cycle considerably. Additionally, even the use of OoA prepregs is not completely ideal from a manufacturing point of view. Heat transfer is still based on convection, which leads to inefficiencies and to spatial gradients in cure and stress due to convective-to-conductive interactions between the oven gas medium (usually air) and the cure materials.<sup>[38–40]</sup> This method drives part-to-part variability, and the fabrication is still limited because of the fixed

geometry of the heating vessel. Given such limitations, the current alternative (i.e., OoA prepregs) needs further improvements to create a viable non-autoclave process addressing the fundamental limitations of the use of an autoclave.

Here, we demonstrate a new non-autoclave process by which it is possible to manufacture aerospace-grade layered advanced composites from conventional autoclave prepregs without either a heating vessel or applied pressure. As presented in **Figure 1a**, prior to a thermal process, a laminate contains voids at the layer/lamina/ply interfaces. Conventionally, laminates are processed with applied pressure ( $P_a$ ) from a pressure vessel (autoclave) to suppress such voids. Alternatively, we found that the capillary pressure from a nanoporous network film replaces the need for applied pressure (from the autoclave) to manufacture void-free layered polymeric architectures (see **Figure 1b,c**). The process comprises the integration of 1) the nanoporous network (i.e., vertically aligned carbon nanotubes (VACNTs) in the current work) into the interlaminar regions of the laminates, and 2) a vacuum-bag-only conductive composite curing process, out-of-oven (OoO) curing<sup>[41–43]</sup> (see Section S2 in the Supporting Information for an overview of the process). The OoO process uses a CNT film as a heating element in contact with the laminate surface such that curing is via conduction rather than convection, eliminating the need for a heating vessel.<sup>[42]</sup> Earlier works have shown that OoO curing enables highly efficient manufacturing of composites from OoA prepregs while preserving thermophysical and mechanical properties (e.g., degree of cure, glass transition temperature, short-beam strength, tensile strength, etc.) observed in the conventional oven curing method.<sup>[42,43]</sup> Autoclave prepregs cured by OoO have not been explored previously because the OoO curing is based on a vacuum-bag-only cure cycle. In prior studies,<sup>[44–49]</sup> it was reported that nanoporous networks such as CNT arrays can draw polymers into itself via capillary-driven wetting. From this phenomenon, we hypothesized that an NPN can be utilized to reduce the extent of interlaminar voids by

enhancing the resin flow into the interlaminar regions (i.e., the capillary pressure from the NPN replaces the applied pressure from an autoclave). Furthermore, such enhanced resin wetting due to capillary pressure was expected to enable the manufacturing of high-quality composites from existing conventional autoclave prepregs in extensive use in many industrial applications, including primary structures in aircraft.

## 2. Results and Discussion

Layered polymeric architectures (hereafter composite) were fabricated via the conventional manufacturing methods (e.g., autoclave or hot-press) as well as the new OoO curing with NPN to explore a non-autoclave process with autoclave prepreg, and to understand underlying mechanisms. Hexcel AS4/8552 unidirectional prepreg was used for this work, which is designed to be cured by an autoclave with vacuum (0.1 MPa) and 0.6–0.7 MPa applied pressure, and is used extensively in the aerospace industry, being one of the few systems extensively characterized and approved by the National Center for Advanced Materials Performance for the entire aerospace industry.<sup>[50]</sup> Three primary types of processing are compared: i) “conventional” curing with applied pressure in an autoclave, ii) conventional curing without applied pressure (“vacuum-only”), and iii) the OoO conductive curing with NPN (“OoO w/ NPN”). Additionally three other process variants (see Section S4 in the Supporting Information) are considered: iv) conventional curing with applied pressure and NPN, v) vacuum-only curing with NPN, and vi) OoO curing without NPN. The conventional composite curing in this study was conducted with an autoclave, comprising a vacuum bag and applied pressure of 0.7 MPa, following the manufacturer’s recommended cure cycle.<sup>[51]</sup> A hot-plate was utilized instead of a heating vessel (e.g., oven) for composite curing without an applied pressure (i.e., vacuum-only curing), in order to avoid spatial gradients in cure due to uncertainty of convective-to-conductive interactions between the convective medium and cure materials.<sup>[38–40]</sup> In the case of OoO curing, vacuum was applied via a vacuum bag without an applied pressure as the OoO curing is originally designed.<sup>[42,43]</sup> Void analysis and short beam shear (SBS) tests were performed so that the mechanical and physical properties of composites cured by each manufacturing condition were compared. SBS testing allows the relatively weak and problematic interlaminar region strength, which is a primary concern in OoA materials and processes, to be directly evaluated. In addition, the underlying mechanisms were explored to understand the results and to suggest further applications.

### 2.1. Void Analysis and Comparison of Mechanical Properties

As discussed in the Introduction, voids at the level of a few percent are associated with significantly reduced composite strength and lifetime. Such voids are introduced into the composite during manufacturing as interlaminar (and sometimes intralaminar) voids. **Figure 2a** shows representative micro-computed tomography ( $\mu$ CT) slices of the three primary processing types. Of note, the secondary manufacturing conditions

are discussed in Section S4 in the Supporting Information to explore mechanisms later in this section. In the X-ray micrographs, the brighter gray-scaled regions denote denser areas such as fibers and polymers, while voids appear as darker. As can be seen in **Figure 2a**, there are no detectable voids in the specimens cured by autoclave (conventional), as expected. By contrast, since vacuum alone is not enough to remove entrapped voids and to suppress the void formation within such materials during curing, the specimens cured without an applied pressure (vacuum-only) resulted in a void fraction of  $\approx 1.65\%$ . Such high void contents of these specimens directly corroborate that applied pressure is required to lower the final void content when curing autoclave prepreg systems. However, when the OoO curing process and NPN were introduced in the interlaminar regions (OoO with NPN), the void content was reduced to the conventional/baseline values, i.e., undetectable. As reported in prior studies of aligned CNT interlaminar reinforcement,<sup>[52–54]</sup> there was no significant difference in the thickness of the interlaminar region before and after the insertion of the aligned CNTs, as observed here. Furthermore, there were no morphological differences such as ply and interlaminar thickness between the OoO with NPN and conventional specimens under high-resolution synchrotron radiation computed tomography (SRCT) images and micrographs. The SRCT images of specimens with NPN cured under different manufacturing conditions are presented in Section S3 in the Supporting Information. The OoO with NPN specimens did not exhibit any detectable voids even though the scans were conducted in a high resolution (voxel size of 650 nm). This is the same result from the specimens cured under the conventional autoclave process (see **Figure S3a,c** in Section S3 in the Supporting Information). **Figure S3b** in the Supporting Information exhibits the representative SRCT slice of the vacuum-only with NPN specimens where all detected voids were located in the intralaminar region, and there were no interlaminar voids, suggesting that the NPN effectively reduces the voids in the interlaminar regions, regardless of the heat input type (hot-plate or OoO). Therefore, NPN effectively eliminates voids in the interlaminar regions as expected, and the integration with the OoO curing enables void-free composite laminates to be manufactured. Furthermore, we observed the same void-free results with another aerospace-grade unidirectional carbon fiber prepreg (Hexcel IM7/8552, designed to be processed in an autoclave<sup>[51]</sup>), which suggests the NPN approach is generalizable to other composites (see Section S9 in the Supporting Information). This is further discussed in the conclusions.

The results of SBS tests were evaluated to compare mechanical properties of the composite laminates cured under different manufacturing conditions. In the SBS test, 10 specimens were examined for each manufacturing process. Even though the short-beam strength may not be directly interpreted as interlaminar shear strength because of mixed failure modes by complex stress distribution,<sup>[55]</sup> it is known that the SBS testing can be utilized to compare composite laminate properties as a screening tool with a description of the failure mode.<sup>[56,57]</sup> **Figure 2b,c** exhibits the short-beam strength of each manufacturing condition. In all cases, the interlaminar shear failure mode was observed. The conventional specimens gave short-beam strength of  $\approx 91$  MPa, which compares

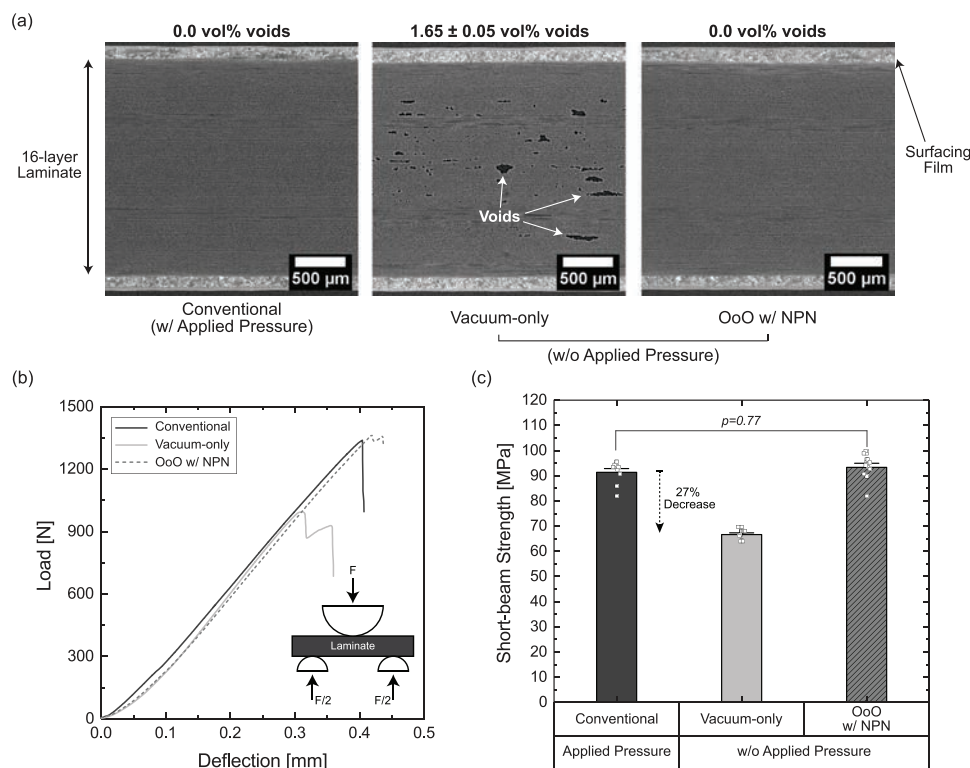


**Figure 2.** Process quality and mechanical properties of layered polymer composites processed via conventional (autoclave with pressure), vacuum-only (oven without pressure), and OoO with NPN introduced in this work: a) Void content and representative  $\mu$ CT cross-sections. Note that in the  $\mu$ CT images, the brighter gray regions denote denser areas such as fibers and polymer, while the voids are imaged as darker gray to black. b) Representative load–deflection curves and c) short-beam strength statistics with standard error. The inset figure in (b) shows the short beam shear test. There is no statistically significant difference between the conventional autoclave-cured materials and the OoO with NPN, and the importance of pressure to both void content and strength is evident from the vacuum-only 27% reduction in strength.

as follows to other relevant systems: it was reported that IM7/8552 laminates have short-beam strengths of  $\approx 118$ <sup>[58]</sup> and  $\approx 93.5$  MPa<sup>[59]</sup> in unidirectional ( $[0]_{32}$ ) and quasi-isotropic ( $[0/90/\pm 45/90/0/\pm 45]_S$ ) layups, respectively. That is, short-beam strength decreased by 20.8% in the quasi-isotropic laminates, when compared to the unidirectional laminates. Given that the short-beam strength of 114.7 MPa reported for AS4/8552 unidirectional ( $[0]_{32}$ ) laminates,<sup>[60]</sup> the short-beam strength of 90.8 MPa can be estimated, which is very close to the measured values of 91 MPa here. By contrast, due to the high void content, the vacuum-only specimens showed  $\approx 27\%$  decrease in the short-beam strength, compared to the conventional and OoO with NPN specimens. Consistent with the extended literature and expectation, matrix-dominated properties are degraded by the existence of voids.<sup>[15–20]</sup> Given that a  $p$ -value less than 0.05 is required to establish a statistical difference with 95% confidence in the Welch's  $t$ -test,<sup>[61]</sup> a  $p$ -value of 0.77 indicated that the means of short-beam strength values of conventional and OoO with NPN specimens were not statistically different from each other. The other secondary processing conditions (i.e., conventional autoclave curing with NPN, vacuum-only hot-plate curing with NPN, OoO without NPN, etc.) provide further insight (see Section S4 in the Supporting Information for the void contents and SBS results of secondary processing conditions). The reduction in void content due to NPN (and the associated strength retention) occurs regardless of

heat application (autoclave, hot-plate, or OoO), and OoO curing showed lower void contents than vacuum-only curing regardless of the presence of NPN. We also observed that the order of manufacturing condition from the highest to the lowest value of short-beam strength matched that from the lowest to the highest value of void content. This observation corroborates the findings from previous studies that high void content can cause detrimental effects on matrix-dominated properties and lifespan of composite parts.<sup>[15–20]</sup> The results of void content and SBS tests suggest that the integration of OoO curing and NPN broadens the options on materials and structural designs, because it enables use of autoclave prepregs to be processed only under vacuum without any modifications to the polymers. Since the material properties of autoclave prepregs have been extensively researched and widely used in industry for decades, the same high-quality composite architectures can be achieved in a much more efficient way (by removing the need for both the time and expense of pressure application).

## 2.2. Nanoporous Network Void Reduction Mechanisms

The formation and growth of voids within a laminate are attributed to mechanically entrapped air, moisture dissolved in the resin, and volatile emission during curing.<sup>[62,63]</sup> Figure 3a shows a 2D synchrotron radiation CT image of an

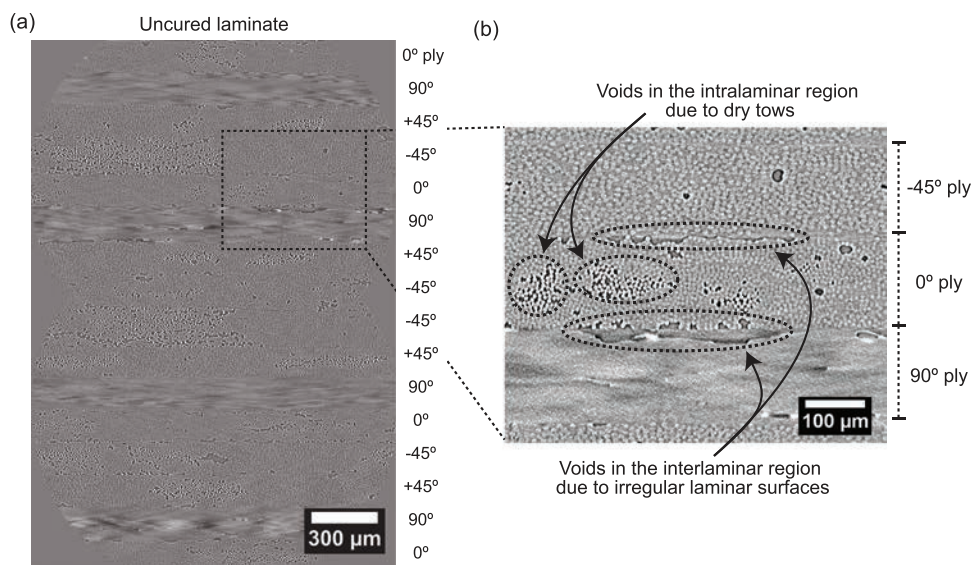


**Figure 3.** Cross-section of an uncured laminate of Hexcel Hexply AS4/8552 [0/90/ ± 45]<sub>2S</sub>: a) representative 2D synchrotron radiation  $\mu$ CT image of the uncured laminate, and b) magnified image of three plies showing entrapped air in the interlaminar due to the irregular lamina surfaces and dry tows in the intralaminar regions.

uncured 16-ply quasi-isotropic laminate. As illustrated in the magnified image (Figure 3b), there are intrinsic void sources in the laminate, which are composed of entrapped air pockets in the interlaminar regions and partially impregnated dry tows in the intralaminar region.<sup>[64]</sup> The intralaminar voids (i.e., partially impregnated dry tows) are most likely to be connected to each other along the microfiber axial direction, and therefore prepregs show a higher permeability along the axial fiber direction than transverse direction.<sup>[65,66]</sup> Hence, most of the intralaminar voids can be removed via vacuum during curing. However, the entrapped voids in the interlaminar region arise from the irregular surfaces of the laminae (see Figure 4); the measured height of peaks and valleys on prepreg surfaces were normally distributed with a standard deviation of  $\approx 5.2 \mu\text{m}$  (see Section S5 in the Supporting Information for the quantified results of the irregular prepreg surfaces). Such interlaminar voids (i.e., entrapped air) may not be connected to each other due to the irregular in-plane distribution and shape of the peaks and valleys. As a result, vacuum is not enough to evacuate the interlaminar voids, and a high-pressure compaction using external pressure (e.g., autoclave) is required to minimize or eliminate the interlaminar voids. This supports other studies that find voids to be typically localized to the interlaminar regions.<sup>[65,67–70]</sup>

Given that the focus of void reduction is in the interlaminar region, we suggest that the effectiveness of the NPN in reducing interlaminar voids is primarily attributed to two features of the NPN: 1) conformability of the NPN to the rough lamina surfaces, and 2) capillary wetting into the aligned nanostructures of the NPN.

### 2.2.1. Conformability of the NPN

During the transfer procedure of NPN to the surfaces of a prepreg, we observed that the NPN tends to conform to the

irregular features on the surface (see Figure 5a–d) of the lamina. To evaluate whether NPN fully conforms, a polydimethylsiloxane (PDMS) replica of the lamina surface was fabricated to allow dark-field microscopy investigation<sup>[71,72]</sup> (see Section S5 in the Supporting Information for the fabrication procedure of replica mold). The PDMS replica was found to be representative of the topography of a lamina via stylus profilometry using a Dektak XT Stylus Profiler (Bruker, USA); see Section S5 in the Supporting Information. Figure 5f is a dark-field microscopy image of the interfaces between an optically transparent PDMS lamina mold and the NPN (i.e., vertically aligned CNT arrays of  $\approx 20 \mu\text{m}$  in height). The lower half of the mold has been covered with NPN, and as presented in the upper part of Figure 5f, the microfeatures of the PDMS mold (i.e., replica of peaks and valleys on the surface of a prepreg) appear bright due to light reflections on the irregular surfaces of microfeatures. However, in the lower part of Figure 5f, the microfeatures were completely filled with the NPN, and present optically as a matte black color without bright reflections. Note that the ability of the NPN to conform to the microscale features of the lamina is consistent with the previous study that individual CNTs within the vertically aligned CNT arrays maintain their vertical orientation without strong interactions between adjacent bundles during a microindentation.<sup>[73]</sup> Moreover, in order to evaluate whether both the top and bottom interfaces of NPN conform, the NPN (i.e., vertically aligned CNT arrays of  $\approx 20 \mu\text{m}$  in height) were sandwiched between two PDMS mold replicas of the lamina surfaces, simulating a laminate layup (see Section S5 in the Supporting Information). Both interfaces were found to be in full contact with the NPN via dark-field microscopy such that there was no bright region observed. Once the microfeatures are filled with NPN, intrinsic void sources do not exist in the interlaminar region due to the NPN contact with the lamina surface. The NPN making contact

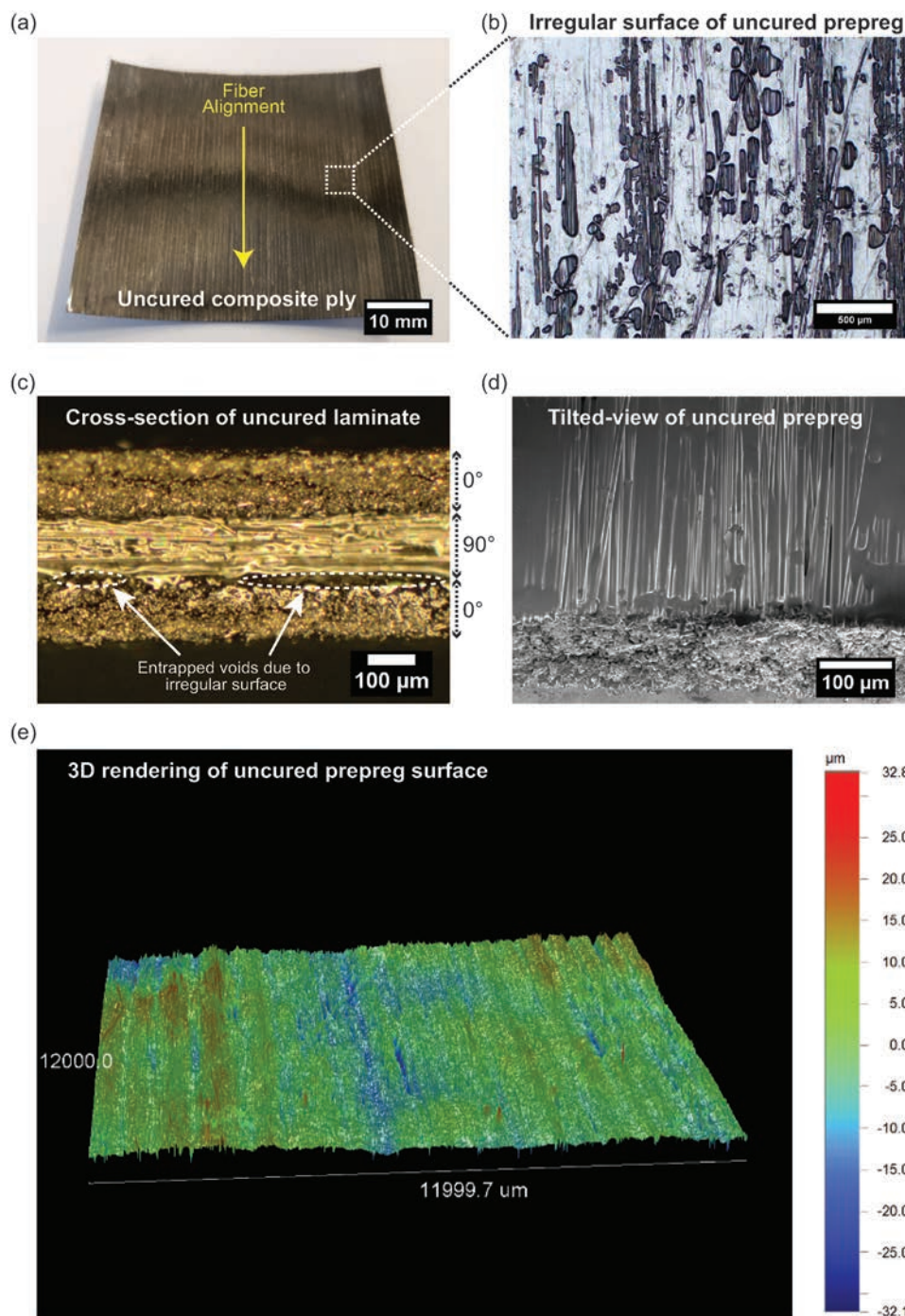


**Figure 4.** Surface roughness of uncured aerospace-grade carbon fiber composite lamina (Hexcel AS4/8552 unidirectional prepreg): a) optical image of the lamina, b) magnified image of the surface of lamina showing roughness, c) cross-section of a laminate ([0/90/0]) showing entrapped voids at the interface due to the irregular surfaces, d) 45° tilted SEM image presenting irregular topography and cross-section of the lamina, and e) exemplary 3D rendering of irregular surface measured by stylus profilometry.

with both lamina allows the strong capillary effect of CNT arrays<sup>[74–78]</sup> to facilitate capillary-driven wetting of polymer throughout the interlaminar region (discussed further in Section 2.2.2). Furthermore, the porous NPN layers are also hypothesized to serve as void extraction pathways as discussed in Section S6 in the Supporting Information.

### 2.2.2. Interlaminar Capillary Pressure Due to the Nanoporous Network

In the curing process of autoclave prepreg laminates, the resin flow velocity is very small compared to infusion processes, corresponding to a low shear rate. Thus, even though the polymer

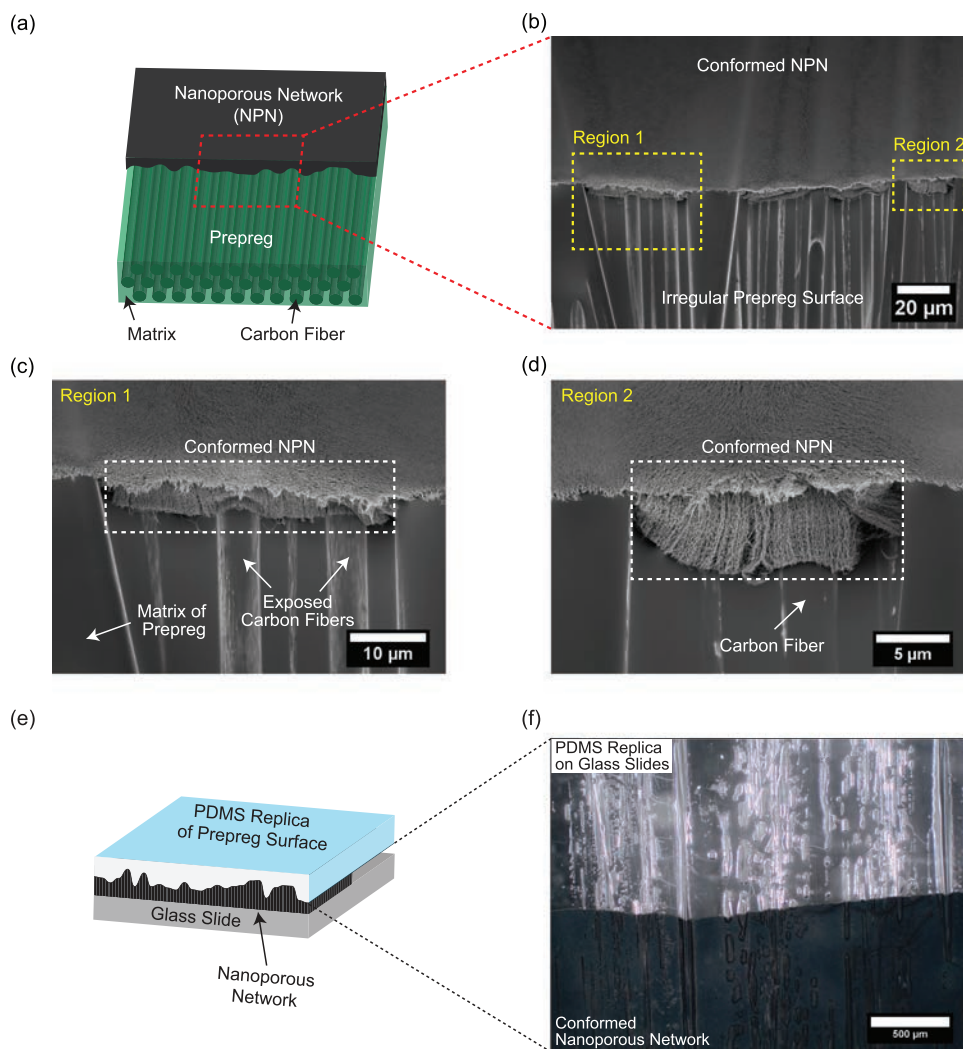


**Figure 5.** Conformability of NPN to lamina: a) Illustration of conformed NPN on a lamina with microscale roughness, b–d) SEM images of NPN conformed to the irregular surface of a lamina, and e) illustration of the PDMS replica mold subjected to dark-field imaging. Note that the lower half of the PDMS mold is covered with NPN, and f) dark-field microscopy image of an optically transparent PDMS mold representing the lamina surface, clearly showing NPN conformability by the dark region in the lower portion of the image.

resins are non-Newtonian fluids, the characteristic flow of the resin during a cure process can be considered as a Newtonian flow because of the low shear rate, which corresponds to very small Reynolds number ( $<0.001$ ).<sup>[79]</sup> At the microscopic scale, the resin flow inside a laminate is modeled by Darcy's law with capillary pressure at the interface between the resin and the gas as follows

$$v = -\frac{\mathbf{K}}{\mu} \nabla P \quad (1)$$

where  $v$ ,  $\mathbf{K}$ ,  $\mu$ , and  $P$  are the flow velocity vector, the permeability tensor, the dynamic viscosity, and the pressure at the flow front, respectively. Based on Equation (1), the direction of the resin flow front into the interlaminar region is given by the sign of the pressure gradient. **Figure 6a** presents the cross-section of the interlaminar region showing the pressure boundary condition when voids are entrapped due to the irregular

prepreg surfaces. At the interface between the resin and entrapped void, the resin pressure ( $P_r$ ) and gas pressure within the entrapped void ( $P_v$ ) give rise to a pressure gradient toward the interlaminar region corresponding to  $\Delta P = P_r - P_v$ . Given that the entrapped voids are generated during the prepreg layup procedure at atmospheric pressure, and are likely to be isolated from each other,  $P_v$  is assumed to be order of 0.1 MPa. In the case of autoclave processing, the applied pressure is  $\approx 0.7$  MPa with partial vacuum of  $\approx 0.02$  MPa additional from the vacuum bag, and hence  $P_r$  of  $\approx 0.72$  MPa is taken. Therefore, the positive pressure gradient in an autoclave toward the interlaminar region ( $\Delta P \approx 0.62$  MPa) suppresses void growth, and further the collapse of voids can occur due to gas diffusion into the heated liquid resin. When only vacuum is applied during curing ( $P_r \leq 0.1$  MPa), the pressure gradient is not sufficient to suppress void growth ( $\Delta P \leq 0$ ), and the entrapped void can even expand/grow due to the thermal expansion of the gas. However, if NPN is introduced into the interlaminar

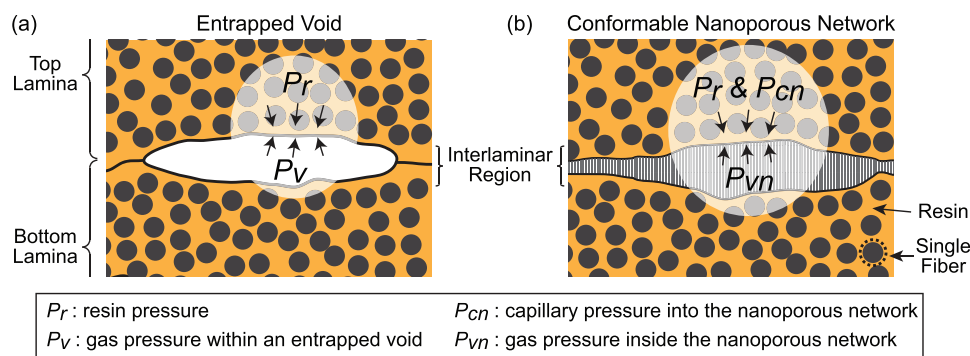


**Figure 6.** Illustration of the pressure boundary condition at the interface (interlaminar region) of composite laminae with: a) entrapped voids due to the irregular surface of prepreg layers, and b) conformable NPN (i.e., vertically aligned carbon nanotube arrays in this work). The drawings are not to scale. The conformable NPN enables capillary-driven polymer wetting into the interface, leading to full polymer impregnation of the interface as observed in this work.

region, capillary pressure from the NPN acts in the same direction as the pressure from the autoclave. Figure 6b illustrates the pressure boundary condition at the interlaminar regions when filled with conformable NPN. It should be noted that the NPN is assumed to have full contact with each lamina surface (Section S5, Supporting Information) and maintains in-plane breathable pathways (Section S6, Supporting Information). At the flow front with NPN, the resin pressure ( $P_r$ ), capillary pressure to the NPN ( $P_{cn}$ ), and gas pressure inside the NPN ( $P_{vn}$ ) give rise to the pressure gradient toward the interlaminar region of  $\Delta P = P_r + P_{cn} - P_{vn}$ . Because a vacuum is drawn under the vacuum bag and the NPN is breathable,  $P_r \approx 0.1$  MPa and  $P_{vn} \approx 0$  MPa are assumed. Similarly,  $P_{cn}$  can be estimated based on morphological characteristics of the CNT arrays and the assumption of 1D resin flow along the fiber alignment<sup>[80–83]</sup> as follows (see Figure 6)

$$P_{cn} = \frac{4}{D_f} \frac{1 - \varepsilon}{\varepsilon} \sigma \cos \theta \quad (2)$$

where  $D_f$ ,  $\varepsilon$ ,  $\sigma$ , and  $\theta$  are diameter of a (nano) fiber, porosity of the NPN, surface tension of the resin, and contact angle between the resin and (nano) fiber, respectively. Given that the NPN comprises aligned nanofibers and has  $D_f \cong 7.8$  nm and  $\varepsilon \cong 0.94$  (see the Experimental Section), the capillary pressure  $P_{cn}$  of  $\approx 1$  MPa is estimated. In addition,  $\sigma \cong 35$  mJ m<sup>-1</sup> and  $\theta \cong 20^\circ$  were used based on known values for similar epoxy system.<sup>[84–86]</sup> As a consequence, a sufficient pressure gradient (relative to the autoclave) toward the interlaminar region ( $\Delta P \approx 1.1$  MPa) is achieved, which is in excess of the autoclave process ( $\Delta P \approx 0.7$  MPa). This high pressure gradient due to NPN capillarity leads to full resin impregnation (full void suppression) at the interlaminar regions such that there are no detectable interlaminar voids. Given the higher pressure, it is possible that the interlaminar regions are consolidated to a greater extent relative to the intralaminar regions, although both the interlaminar and intralaminar regions have no detectable voids. Finally, since any nanoporous architectures having sufficiently strong capillary pressure to draw polymer matrix into the interlaminar region can be utilized for the capillary approach, future studies should explore alternative NPN materials to expand the versatility of this approach.

### 3. Conclusion

A capillary approach utilizing NPNs to process layered polymeric architectures is presented and demonstrated, which addresses the limitations of current manufacturing methods such as autoclave and out-of-autoclave prepreg processes. This technique entails the integration of the recently proposed OoO curing process, and the insertion of a nanoporous network (i.e., vertically aligned carbon nanotube arrays in the current work) into the interlaminar regions of layered polymeric architectures. In essence, capillary pressure replaces autoclave pressure that is needed to remove voids from the interlaminar region of the laminates. The laminates comprising conventional autoclave-required aerospace-grade prepreps were processed by the OoO with NPN technique, and physical properties were examined to compare with conventionally cured laminates. The processed composites had <0.1% volume of voids (commensurate with autoclave-processed composites) without using either a heating vessel or applied pressure, and mechanical testing shows that interlaminar strength (via short beam shear) is maintained. We found that the underlying mechanisms consist of: 1) conformability of the nanoporous network that eliminates entrapped voids due to the irregular surface profile of the lamina; 2) enhanced polymer wetting into the interlaminar regions due to strong capillary pressure of the NPN utilized herein. The technique proposed here for autoclave prepreg includes the same noted advantages for the OoO process utilizing OoA prepreg. Additionally, as the technique allows the oven and pressure vessel to be eliminated, it enables expanded advantages as follows: 1) the wide range of existing autoclave prepreg material in use with already-proven mechanical properties are now available in an OoA environment, 2) removal of size and shape constraints on composite components using a scalable OoO heating element, and 3) cost savings on manufacturing by efficient thermal processing via OoO curing. Moreover, the process can be combined together with conventional composite manufacturing processes such as resin infusion, and may contribute to the design and manufacturing of defect-free advanced composite architectures, while adding new or improved capabilities such as cure sensing, reduction in part-to-part variation, and the ability to cure uniformly in regions with large local geometric variations. In addition, this capillary pressure approach

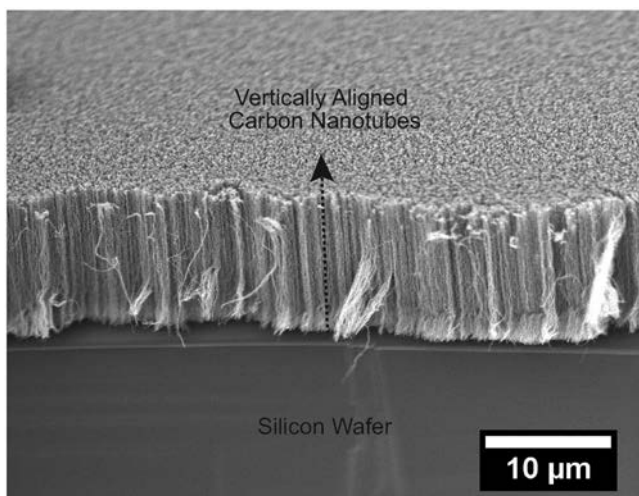


**Figure 7.** 45° tilted SEM image of  $\approx 20\ \mu\text{m}$  vertically aligned carbon nanotube arrays (NPN as used herein) grown by a thermal catalytic chemical vapor deposition process on a silicon wafer.

is anticipated to be applied to many manufacturing applications where the need for high applied pressure are limiting, such as press forming, closed-mold resin infusion processing, and adhesive joining.

#### 4. Experimental Section

**Synthesis of VACNTs as NPN:** VACNT synthesis (used here as the NPN) proceeded via a thermal catalytic chemical vapor deposition process with a quartz tube furnace of 44 mm inner diameter at atmospheric pressure, which was similar to a previously reported process.<sup>[42,49,87,88]</sup> Ethylene was used as the carbon source, and water of 600 ppm was added to the helium gas. The as-grown CNT arrays consisted of multiwalled CNTs having 3–7 walls<sup>[89]</sup> with an average inner and outer diameter of  $\approx 5.1$  and  $\approx 7.8$  nm, respectively. The volume fraction of CNT arrays corresponded to  $\approx 1.6\%$  with intrinsic CNT density of  $\approx 1.6\ \text{g cm}^{-3}$  and average inter-CNT spacing of  $\approx 59$  nm. Also, the as-grown CNT arrays with a height of  $\approx 20\ \mu\text{m}$  were used for NPN (see **Figure 7**). Given that the  $20\ \mu\text{m}$  tall NPNs were compressed to  $\approx 5\ \mu\text{m}$  in the interlaminar region, the effective volume fraction of NPN for

capillary pressure corresponded to  $\approx 6\%$ , which resulted in the porosity of NPN of  $\approx 94\%$ . The CNT heaters for OoO curing were fabricated via roller densification of the CNT arrays having the height of  $\approx 500\ \mu\text{m}$ , similar to a previous study.<sup>[42]</sup>

**Composite Fabrication and Processing:** Hexcel AS4/8552 aerospace-grade unidirectional carbon fiber prepreg was used, which is designed to be processed in an autoclave.<sup>[51]</sup> The nominal cured ply thickness of this prepreg is  $130\ \mu\text{m}$  with a target volume fraction of 63.5% of carbon fiber in each ply. Considering the standards used for the experiments, 16 plies (nominal laminate thickness of 2.08 mm) were used for the laminates in a quasi-isotropic layup of  $[0/90/\pm 45]_{2s}$ . In the case of laminates with NPN at the interlaminar region, CNT arrays with a height of  $\approx 20\ \mu\text{m}$  were introduced to all 15 interlaminar regions within 16-ply laminates by manual transfer onto the surface of each prepreg, following the previously reported procedures.<sup>[49,53]</sup> Of note, the void results with partially introduced NPN are presented in Section S9 in the Supporting Information; NPNs significantly reduced the voids in the interlaminar regions only where they were installed, further underscoring the capillary pressure effect. To fabricate the CNT heaters for OoO curing, the fabrication methods in the previous study were followed using Cu mesh (Dexmet 2CU4-100FA) and composite surfacing films (TenCate Advanced Composites TC235-1SF).<sup>[41,42]</sup> It should be noted that the manufactured CNT heaters were attached on the top and bottom surfaces of all prepared 16-ply laminates so that all laminates maintained a symmetric layup even though only one heater was used (electrically activated) for OoO curing.

For the conventional autoclave curing process, the recommended cure procedure from the prepreg manufacturer was followed using an autoclave<sup>[51]</sup>: cure temperature of  $110\ ^\circ\text{C}$  with a hold time of 60 min, and then cure temperature of  $180\ ^\circ\text{C}$  with a hold time of 120 min; ramp rate at  $3\ ^\circ\text{C min}^{-1}$ ; autoclave gauge pressure of 0.6 MPa with a vacuum. For the vacuum-only (i.e., oven or hot-plate) curing process, the same vacuum bagging procedure for the autoclave process above was used. Once a vacuum bag was prepared for the cure, the laminate and cure materials were placed on a programmable hot-plate (EchoTherm HS60A) for curing. During the cure cycle, the same curing condition in the technical data sheet was followed without the applied pressure of 0.7 MPa. For OoO curing, the cure setup in the previous study was used (see **Figure 8** for the vacuum bagging setup with two-sided heaters).<sup>[43]</sup> Also, thermal insulating blocks (25 mm thick ZIRCAR Ceramics Inc. MICROSIL Microporous Insulation) were installed to reduce heat loss to the environment. During a cure cycle, only one heater was utilized as a heating element since the one-sided heater is enough to cure a  $\approx 2$  mm thick 16-ply laminate.<sup>[41–43]</sup> A DC power supply was connected to the two copper tape electrodes of the heater to control the input voltage to follow the specific cure cycle. The vacuum bagging setup was placed on a lab bench, and the temperature was measured by a thermocouple (OMEGA Engineering fast-response K-type) that was attached to the heater.

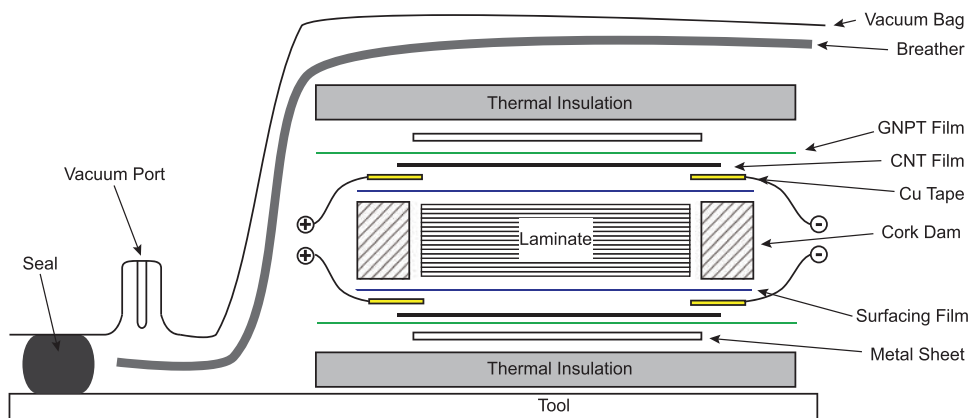


**Figure 8.** Vacuum bag layout of the OoO curing process with two-sided heaters. Two carbon nanotube (CNT) heaters were installed directly on the top and bottom surface of all laminates, although in the OoO curing only the top surface heater is used (electrically activated) as a heating element.

***μCT Imaging and Void Analysis:*** μCT imaging of laminates was performed with Nikon Metrology XT H 225 ST at the Center for Nanoscale Systems, Harvard. An isotropic voxel size of 3.3 μm was acquired with the X-ray beam energy of 80 kV and 70 μA. Molybdenum was used as the X-ray source with the reflection target mode. For each scan, 1500 2D projections were captured while a specimen was rotated in 180°. The exposure time for each projection was 1 s, and the projection radiographs were reconstructed using the embedded software in the μCT machine, and reconstructed 3D volumes were analyzed with the commercial visualization software, VGStudio MAX 3.0, to acquire 2D slices. High-resolution synchrotron radiation CT images were acquired at the ID-19 beamline at the European Synchrotron Radiation Facility (ESRF) in Grenoble, France. An isotropic voxel size of 650 nm was used for synchrotron radiation CT images. The void content of cured laminates was evaluated by μCT following ASTM E1441. From a manufacturing point of view, it is important to understand the impact of the location and size of void defects on the structural performance of composites, including strength and fatigue behavior. Therefore, μCT-based assessment is a way to acquire the 3D distribution of voids. After collecting raw μCT images, the void content can be easily calculated by applying a threshold filter.

***Short Beam Shear Test:*** The short beam shear test was conducted based on ASTM standard D2344, which is also consistent with DIN EN2563. The dimension of a specimen was nominally 12 mm × 4 mm × 2 mm ( $L \times W \times t$ ), and these specimens were taken from the 60 mm × 50 mm quasi-isotropic laminates ( $[0/90/\pm 45]_{2S}$ ) comprising 16 plies of AS4/8552 prepreg. The cut laminate edges were polished with 800, 1200, and 2400 grit sandpapers to avoid rough or uneven surfaces which may result in predamage at the edges. As prescribed in the ASTM standard D2344,<sup>[90]</sup> a three-point bend fixture with a loading nose of 6 mm, supports of 3 mm diameter steel cylinders, and the span length of 8 mm were used. During the tests, the force applied to the specimen was monitored at a rate of cross-head movement of 1.0 mm min<sup>-1</sup> applied by a Zwick/Roell Z010 mechanical testing machine. The short-beam strength was then calculated using Equation (3) as follows

$$\sigma_{SBS} = 0.75 \times \frac{P_f}{w \times t} \quad (3)$$

where  $P_f$ ,  $w$ , and  $t$  are the load at the failure observed during the test, the width, and the thickness of the specimen, respectively.

## Supporting Information

Supporting Information is available from the Wiley Online Library or from the author.

## Acknowledgements

This work was supported by Airbus, ANSYS, Embraer, Lockheed Martin, Saab AB, Saertex, and Teijin Carbon America through MIT's Nano-Engineered Composite aerospace Structures (NECST) Consortium. This work made use of the facilities at the Institute for Soldier Nanotechnologies at MIT, supported (in part) by the U.S. Army Research Laboratory and the U.S. Army Research Office through the Institute for Soldier Nanotechnologies, under contract number W911NF-13-D-0001. The SRCT experiments were performed on beamline ID-19 at the European Synchrotron Radiation Facility (ESRF), Grenoble, France. This work was performed in part at the Center for Nanoscale Systems (CNS) at Harvard University, and supported (in part) by the U.S. Army Natick Soldier R, D&E Center (NSRDEC). J.L. acknowledges support from Kwangjeong Educational Foundation. The authors kindly thank Saab AB for donation of the autoclave prepreg, and Profs. David Hardt, Gareth McKinley, and John Hart (MIT) for helpful technical discussion.

## Conflict of Interest

The authors declare no conflict of interest.

## Keywords

capillary, carbon nanotubes, composite manufacturing, conductive curing, nanoporous network, void

Received: August 15, 2019

Revised: October 25, 2019

Published online:

- [1] J.-J. Luo, I. M. Daniel, *Compos. Sci. Technol.* **2003**, *63*, 1607.
- [2] F. Hussain, M. Hojjati, M. Okamoto, R. E. Gorga, *J. Compos. Mater.* **2006**, *40*, 1511.
- [3] J. N. Coleman, U. Khan, W. J. Blau, Y. K. Gun'ko, *Carbon* **2006**, *44*, 1624.
- [4] P.-C. Ma, N. A. Siddiqui, G. Marom, J.-K. Kim, *Composites, Part A* **2010**, *41*, 1345.
- [5] Y. Liang, D. Wu, X. Feng, K. Müllen, *Adv. Mater.* **2009**, *21*, 1679.
- [6] E. P. Giannelis, *Adv. Mater.* **1996**, *8*, 29.
- [7] Y. Ji, Y. Y. Huang, R. Rungsawang, E. M. Terentjev, *Adv. Mater.* **2010**, *22*, 3436.
- [8] S. Schymura, M. Kühnast, V. Lutz, S. Jagiella, U. Dettlaff-Weglikowska, S. Roth, F. Giesselmann, C. Tschierske, G. Scalia, J. Lagerwall, *Adv. Funct. Mater.* **2010**, *20*, 3350.
- [9] S. C. Jana, S. Jain, *Polymer* **2001**, *42*, 6897.
- [10] F. C. Campbell Jr., *Manufacturing Technology for Aerospace Structural Materials*, Elsevier, Amsterdam **2011**.
- [11] C. E. Harris, J. H. Starnes Jr., M. J. Stuart, *An Assessment of the State-of-the-Art in the Design and Manufacturing of Large Composite Structures for Aerospace Vehicles*, Technical Report, **2001**.
- [12] L. Farhang, *Ph.D. Thesis*, University of British Columbia **2014**.
- [13] *Manufacturing Techniques for Polymer Matrix Composites (PMCs)* (Eds: S. G. Advani, K.-T. Hsiao), Woodhead Publishing Series in Composites Science and Engineering, Woodhead Publishing, Cambridge **2012**.
- [14] S. Mazumdar, *Composites Manufacturing: Materials, Product, and Process Engineering*, CRC Press, Boca Raton, FL **2001**.
- [15] P. Olivier, J. P. Cottu, B. Ferret, *Composites* **1995**, *26*, 509.
- [16] S. R. Ghiorse, *SAMPE Q.* **1993**, *24*, 54.
- [17] H. Zhu, B. Wu, D. Li, D. Zhang, Y. Chen, *J. Mater. Sci. Technol.* **2011**, *27*, 69.
- [18] L. Liu, B.-M. Zhang, D.-F. Wang, Z.-J. Wu, *Compos. Struct.* **2006**, *73*, 303.
- [19] A. R. Chambers, J. S. Earl, C. A. Squires, M. A. Suhot, *Int. J. Fatigue* **2006**, *28*, 1389.
- [20] N. C. W. Judd, W. W. Wright, *SAMPE J.* **1978**, *14*, 10.
- [21] T. G. P. Gutowski, *Advanced Composites Manufacturing*, John Wiley & Sons, New York **1997**.
- [22] D. Abliz, D. Yugang, L. Steuernagel, X. Lei, L. Dichen, G. Ziegmann, *Polym. Polym. Compos.* **2013**, *21*, 341.
- [23] G. Gardiner, *High-Perform. Compos.* **2011**, *19*, 32.
- [24] T. Centea, L. K. Grunenfelder, S. R. Nutt, *Composites, Part A* **2015**, *70*, 132.
- [25] L. K. Grunenfelder, S. R. Nutt, presented at *43rd Int. SAMPE Tech Conf.*, Fort Worth, Texas, October **2011**.
- [26] B. Louis, K. Hsiao, G. Fernlund, in *54th Int. SAMPE Symp. and Exhibition* (Eds: R. Albers, P. Hubert, S. W. Beckwith), Seattle, Washington, USA, May **2010**, pp. 17–20.
- [27] M. Wysocki, R. Larsson, S. Toll, *Proc. of the 17th Int. Conf. on Composite Materials*, Edinburgh, UK, July **2009**.

- [28] C. Ridgard, presented at *Proc. of the SAMPE 2009 Conf.*, Baltimore, MD, May **2009**.
- [29] L. Repecka, J. Boyd, *Proc. of the SAMPE 2002 Conf.*, Long Beach, California, USA, May **2002**.
- [30] L. K. Grunenfelder, T. Centea, P. Hubert, S. R. Nutt, *Composites, Part A* **2013**, 45, 119.
- [31] L. Fahrang, G. Fernlund, *Proc. of the SAMPE 2011 Conf.*, Long Beach, California, USA, May **2011**.
- [32] T. Centea, S. R. Nutt, *J. Compos. Mater.* **2015**, 50, 2305.
- [33] R. A. Witik, F. Gaille, R. Teuscher, H. Ringwald, V. Michaud, J.-A. E. Manson, *J. Cleaner Prod.* **2012**, 29–30, 91.
- [34] S. Thomas, S. R. Nutt, *Appl. Compos. Mater.* **2009**, 16, 183.
- [35] G. F. Xu, L. Repecka, S. Mortimer, S. Peake, J. Boyd, *Manufacture of void-free laminates and use thereof, US6391436B1* **2002**.
- [36] M. Brilliant, *M.Eng. Thesis*, McGill University, Montreal, Canada **2010**.
- [37] G. G. Bond, J. M. Griffith, G. L. Hahn, C. Bongiovanni, J. Boyd, *SAMPE J.* **2009**, 45, 6.
- [38] P. F. Monaghan, M. T. Brogan, *Compos. Manuf.* **1991**, 2, 233.
- [39] Q. Wang, L. Wang, W. Zhu, Q. Xu, Y. Ke, *J. Reinf. Plast. Compos.* **2017**, 36, 1564.
- [40] N. Kluge, T. Lundstrom, A. L. Ljung, L. Westerberg, T. Nyman, *J. Reinf. Plast. Compos.* **2016**, 35, 566.
- [41] J. Lee, *Ph.D. Thesis*, Massachusetts Institute of Technology **2014**.
- [42] J. Lee, I. Y. Stein, S. S. Kessler, B. L. Wardle, *ACS Appl. Mater. Interfaces* **2015**, 7, 8900.
- [43] J. Lee, X. Ni, F. Daso, X. Xiao, D. King, J. S. Gómez, T. B. Varela, S. S. Kessler, B. L. Wardle, *Compos. Sci. Technol.* **2018**, 166, 150.
- [44] K. Shin, S. Obukhov, J.-T. Chen, J. Huh, Y. Hwang, S. Mok, P. Dobriyal, P. Thiyagarajan, T. P. Russell, *Nat. Mater.* **2007**, 6, 961.
- [45] J. Cai, E. Perfect, C.-L. Cheng, X. Hu, *Langmuir* **2014**, 30, 5142.
- [46] M. R. Stukan, P. Ligneul, J. P. Crawshaw, E. S. Boek, *Langmuir* **2010**, 26, 13342.
- [47] M. Zhang, P. Dobriyal, J.-T. Chen, T. P. Russell, J. Olmo, A. Merry, *Nano Lett.* **2006**, 6, 1075.
- [48] D. I. Dimitrov, A. Milchev, K. Binder, *Phys. Rev. Lett.* **2007**, 99, 54501.
- [49] B. L. Wardle, D. S. Saito, E. J. Garcia, a. J. Hart, R. G. de Villoria, E. A. Verploegen, *Adv. Mater.* **2008**, 20, 2707.
- [50] National Center for Advanced Materials Performance.
- [51] Hexcel, HexPly 8552 product data sheet.
- [52] J. Blanco, E. J. Garcia, R. G. de Villoria, B. L. Wardle, *J. Compos. Mater.* **2009**, 43, 825.
- [53] D. Lewis, B. L. Wardle, in *56th AIAA/ASCE/AHS/ASC Structures, Structural Dynamics, and Materials Conf.*, AIAA SciTech Forum, American Institute of Aeronautics and Astronautics, Kissimmee, Florida, USA, January **2015**.
- [54] E. Kalfon-Cohen, D. Lewis, J. Ravine, B. L. Wardle, in *57th AIAA/ASCE/AHS/ASC Structures, Structural Dynamics, and Materials Conf.*, San Diego, California, USA, January **2016**.
- [55] B. K. Daniels, N. K. Harakas, R. C. Jackson, *Fibre Sci. Technol.* **1971**, 3, 187.
- [56] C. Berg, J. Tirosh, M. Israeli, in *Analysis of Short Beam Bending of Fiber Reinforced Composites* (Ed: H. Corten), Vol. 497, ASTM International, West Conshohocken, PA **1972**, pp. 206–218.
- [57] DIN EN 2563, *British Standard Aerospace Series - Carbon Fibre Reinforced Plastics - Unidirectional Laminates; Determination of the Apparent Interlaminar Shear Strength*, German Institute for Standardisation, Berlin, Germany **1997**.
- [58] K. Marlett, Y. Ng, J. Tomblin, *Test Report CAM-RP-2009-015, Rev. A*, National Center for Advanced Materials Performance, Wichita, KS **2011**, pp. 1–238.
- [59] D. J. Lewis, *Ph.D. Thesis*, Massachusetts Institute of Technology **2016**.
- [60] K. Marlett, Y. Ng, J. Tomblin, *Hexcel 8552 AS4 Unidirectional Prepreg 190 gsm @ 35% RC Qualification Material Property Data Report*, Technical Report, **2011**.
- [61] B. L. Welch, *Biometrika* **1947**, 34, 28.
- [62] L. K. Grunenfelder, S. R. Nutt, *Compos. Sci. Technol.* **2010**, 70, 2304.
- [63] J. Kardos, M. Duduković, R. Dave, *Adv. Polym. Sci.* **1986**, 80, 101.
- [64] A. Arafath, G. Fernlund, A. Poursartip, presented at *Proc. of the 17th Int. Conf. on Composite Materials (ICCM-17)*, Edinburg, Scotland, July **2009**.
- [65] S. Hernández, F. Sket, J. M. Molina-Aldareguí a, C. González, J. Llorca, *Compos. Sci. Technol.* **2011**, 71, 1331.
- [66] S. Hernández, F. Sket, C. González, J. Llorca, *Compos. Sci. Technol.* **2013**, 85, 73.
- [67] H. Huang, R. Talreja, *Compos. Sci. Technol.* **2005**, 65, 1964.
- [68] Z. Gurdal, A. Tomasino, S. B. Biggers, *SAMPE J.* **1991**, 27, 39.
- [69] D. K. Hsu, K. M. Uhl, in *Review of Progress in Quantitative Non-destructive Evaluation* (Eds: D. O. Thompson, D. E. Chimenti), Springer US, Boston, MA **1987**, pp. 1175–1184.
- [70] C. A. Howe, R. J. Paton, A. A. Goodwin, in *11th Proc. of ICCM*, Vol. 11, Gold Coast, Australia, July **1997**.
- [71] L. Gitlin, P. Schulze, D. Belder, *Lab Chip* **2009**, 9, 3000.
- [72] M. W. Toepke, D. J. Beebe, *Lab Chip* **2006**, 6, 1484.
- [73] M. R. Maschmann, Q. Zhang, R. Wheeler, F. Du, L. Dai, J. Baur, *ACS Appl. Mater. Interfaces* **2011**, 3, 648.
- [74] E. J. Garcia, B. L. Wardle, A. J. Hart, N. Yamamoto, *Compos. Sci. Technol.* **2008**, 68, 2034.
- [75] N. Chakrapani, B. Wei, A. Carrillo, P. M. Ajayan, R. S. Kane, *Proc. Natl. Acad. Sci. USA* **2004**, 101, 4009.
- [76] D. N. Futaba, K. Hata, T. Yamada, T. Hiraoka, Y. Hayamizu, Y. Kakudate, O. Tanaike, H. Hatori, M. Yumura, S. Iijima, *Nat. Mater.* **2006**, 5, 987.
- [77] X. H. Haur, J. J. Zhou, E. Sansom, M. Gharib, S. Chornng, *Nanotechnology* **2007**, 18, 305301.
- [78] H. Liu, J. Zhai, L. Jiang, *Soft Matter* **2006**, 2, 811.
- [79] C. Park, in *Advances in Composites Manufacturing and Process Design* (Ed: P. Boisse), Woodhead Publishing, Cambridge **2015**, pp. 317–378.
- [80] K. J. Ahn, J. C. Seferis, J. C. Berg, *Polym. Compos.* **1991**, 12, 146.
- [81] S. Chwastiak, *J. Colloid Interface Sci.* **1973**, 42, 298.
- [82] J. G. Williams, C. E. Morris, B. C. Ennis, *Polym. Eng. Sci.* **1974**, 14, 413.
- [83] S. C. Amico, C. Lekakou, *Polym. Compos.* **2002**, 23, 264.
- [84] S. A. Page, R. Mezzenga, L. Boogh, J. C. Berg, J.-A. E. Manson, *J. Colloid Interface Sci.* **2000**, 222, 55.
- [85] K. Grundke, P. Uhlmann, T. Gietzelt, B. Redlich, H.-J. Jacobasch, *Colloids Surf. A* **1996**, 116, 93.
- [86] M. Hautier, D. Lévêque, C. Huchette, P. Olivier, *Plast., Rubber Compos.* **2010**, 39, 200.
- [87] A. M. Marconnet, N. Yamamoto, M. A. Panzer, B. L. Wardle, K. E. Goodson, *ACS Nano* **2011**, 5, 4818.
- [88] J. Lee, I. Y. Stein, M. E. Devoe, D. J. Lewis, N. Lachman, S. S. Kessler, S. T. Buschhorn, B. L. Wardle, *Appl. Phys. Lett.* **2015**, 106, 053110.
- [89] A. J. Hart, A. H. Slocum, *J. Phys. Chem. B* **2006**, 110, 8250.
- [90] *ASTM-D2344*, ASTM International, West Conshohocken, PA **2006**.

**ADVANCED  
MATERIALS**  
INTERFACES

Supporting Information

for *Adv. Mater. Interfaces*, DOI: 10.1002/admi.201901427

Void-Free Layered Polymeric Architectures via Capillary-  
Action of Nanoporous Films

*Jeonyoon Lee, Seth S. Kessler, and Brian L. Wardle\**

---

**FULL PAPER**

Advanced Materials Interfaces

# Supporting Information: Void-free Layered Polymeric Architectures *via* Capillary-action of Nanoporous Films

Jeonyoon Lee<sup>1\*</sup> | Seth S. Kessler<sup>2</sup> | Brian L. Wardle<sup>1</sup>

<sup>1</sup>Department of Aeronautics and Astronautics, Massachusetts Institute of Technology, Cambridge, Massachusetts 02139, United States

<sup>2</sup>Metis Design Corporation, Boston, Massachusetts 02114, United States

## Correspondence

Brian L. Wardle, Department of Aeronautics and Astronautics, Massachusetts Institute of Technology, Cambridge, Massachusetts 02139, United States  
Email: wardle@mit.edu

## Funding information

## S1 | PRESENCE OF VOIDS WITHIN COMPOSITE LAMINATES PROCESSED WITHOUT APPLIED AUTOCLAVE PRESSURE

Figure S1 shows the results of curing autoclave prepregs (Hexcel Hexply AS4/8552 in a  $[0/90/\pm 45]_{25}$  layup) by an oven without applied pressure. The laminate shown here was cured with vacuum but without an applied pressure. Due to insufficient pressure to suppress void formation, the laminate cured without an applied pressure shows a significant amount ( $\sim 5.0\%$ ) of voids. The brighter gray-scaled regions denote denser areas such as fibers and polymer matrix, while the voids appear as darker gray-scaled regions. In addition to the cross-section, Figure S1b exhibits a 3D rendering of voids (shown in gray) within the laminate. Such a high void content emphasizes the need for an applied pressure (e.g., autoclave). The presence of voids within composite laminates causes detrimental effects on structural performance and lifespan of composite parts [1–6].

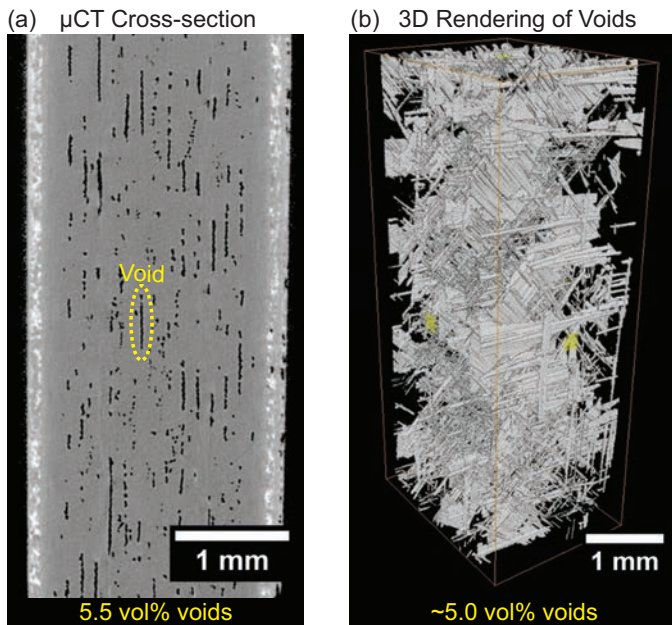


**FIGURE S1** Composite laminate comprised of autoclave prepreg (Hexcel Hexply AS4/8552 in a  $[0/90/\pm 45]_{25}$  layup,  $130\ \mu\text{m}$  nominal ply thickness) processed in an oven without an applied pressure. (a) X-ray microtomography showing cross-section of a laminate with dark regions indicating voids, and (b) 3D rendering of voids where now the voids are shown in gray.

## S2 | OVERVIEW OF THE NON-AUTOCCLAVE CAPILLARY-ENHANCED PROCESS

The non-autoclave capillary-enhanced process (out-of-oven curing with NPN) consists of the integration of: (1) insertion of nanoporous network (i.e., vertically aligned carbon nanotube arrays in the current work) into the interlaminar regions of composite laminates, and (2) the vacuum-bag-only conductive composite curing process, out-of-oven (OoO) curing [7–9]. Figure S2 shows the schematics of the process. The OoO process (see Figure S2b) uses a carbon nanotube (CNT) film as a heating element directly integrated onto the surface of a laminate with a surfacing film such that the curing process does not require any heating vessel or convective medium [8]. As presented in Figure S2c, a nanoporous network (NPN) comprised of VACNTs is inserted in the interlaminar regions of composite laminate. The capillary flow of polymer from the prepreg into nanoporous media is utilized to reduce the extent of interlaminar voids by drawing the resin into the interlaminar regions.

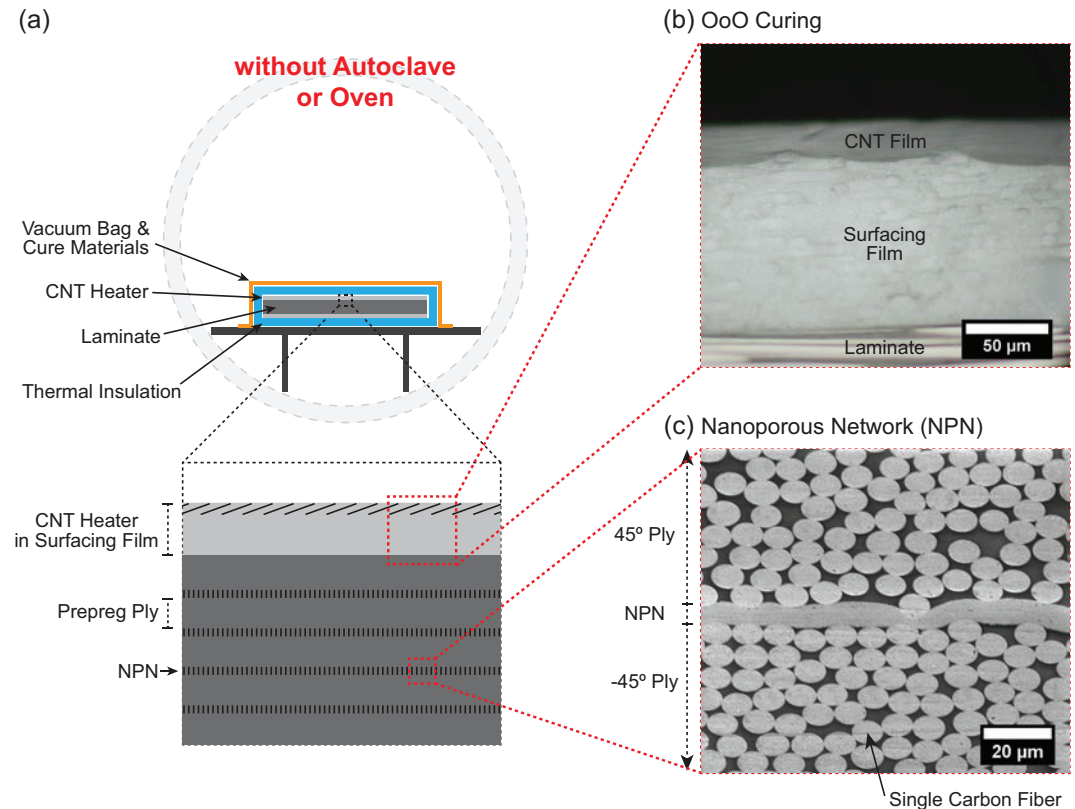


**FIGURE S2** Non-autoclave process (out-of-oven curing with NPN) for conventional autoclave prepregs. (a) Schematics of the process comprised of out-of-oven (OoO) curing and introduction of nanoporous networks (NPN), and micrographs of: (b) a CNT film heater for out-of-oven conductive curing, and (c) nanoporous network (i.e., vertically aligned CNT arrays) introduced in the interlaminar region.

### S3 | COMPARISON OF LAMINATE MORPHOLOGIES

Figure S3 presents synchrotron radiation CT (SRCT) images of specimens with NPN cured under different manufacturing conditions. SRCT imaging was conducted at the ID-19 beamline at the European Synchrotron Radiation Facility (ESRF) in Grenoble, France. As can be seen in Figure S3c, the OoO with NPN specimens did not exhibit any detectable voids even though the scans were conducted at high resolution (voxel size of 650 nm). This is the same result from the specimens cured under the conventional autoclave process, and there was no detectable morphological difference between the OoO with NPN and conventional autoclave processing with NPN specimens (see Figure S3a and c). Figure S3b is a representative slice of the vacuum-only with NPN specimens. All detected voids in this specimen were located in the intralaminar region, and there were no interlaminar voids. The observation suggests that the NPN effectively reduces the voids in the interlaminar regions, regardless of the heat input type (hot plate or OoO). That is, when we introduced NPN into the laminate and cured it under hot plate vacuum-only conditions, there was no interlaminar voids but some intralaminar voids. Therefore, we conclude that NPN significantly helps to reduce the voids especially in the interlaminar regions, and integration with the OoO curing enables fully void-free composite laminates to be manufactured.

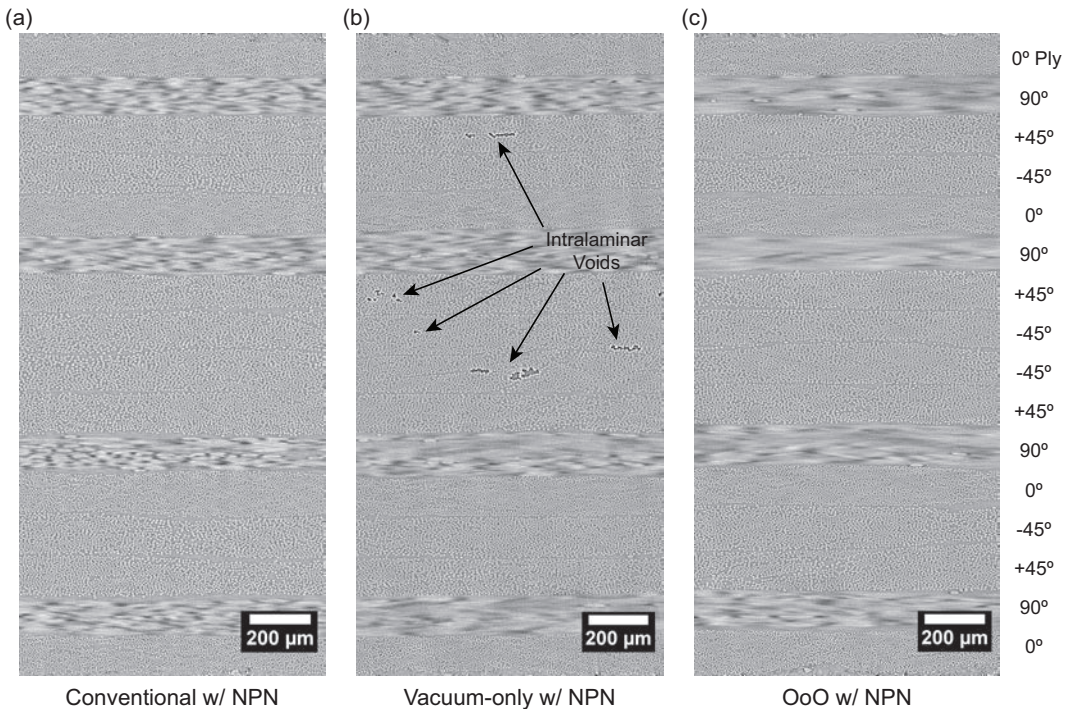


**FIGURE S3** Representative synchrotron radiation CT images of autoclave-formulated prepreg laminates (Hexcel Hexply AS4/8552 in a  $[0/90/\pm 45]_{2S}$  layup) under different types of curing: (a) conventional autoclave-cured with NPN specimen, (b) vacuum-only with NPN specimen on hot plate, and (c) OoO with NPN specimen. There was no morphological difference noted qualitatively between the interlaminar regions.

## S4 | ADDITIONAL RESULTS ON SHORT-BEAM STRENGTH AND VOID CONTENT

The other possible variations of manufacturing condition (i.e., conventional autoclave curing with NPN, vacuum-only hot-plate curing with NPN, OoO without NPN) were also conducted. Figure S4 shows the short-beam strengths and void content for all manufacturing conditions. From the void analysis and mechanical testing, we observed two phenomena by comparing manufacturing conditions: (1) introduction of NPN resulted in a reduction of the total amount of porosity within a laminate; (2) the OoO curing resulted in a lower void content than vacuum-only hot-plate curing. Also, these two phenomena were independent in that an insertion of NPN reduced the void content regardless of heat application (autoclave, hot plate, or OoO), and OoO curing showed lower void contents than vacuum-only

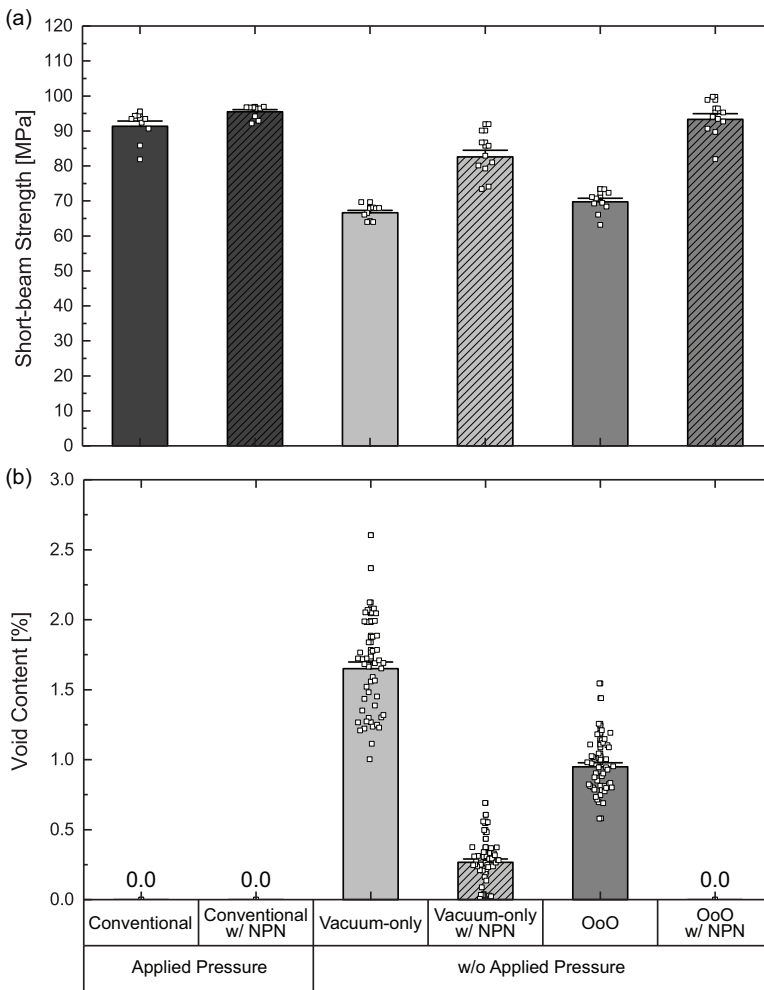
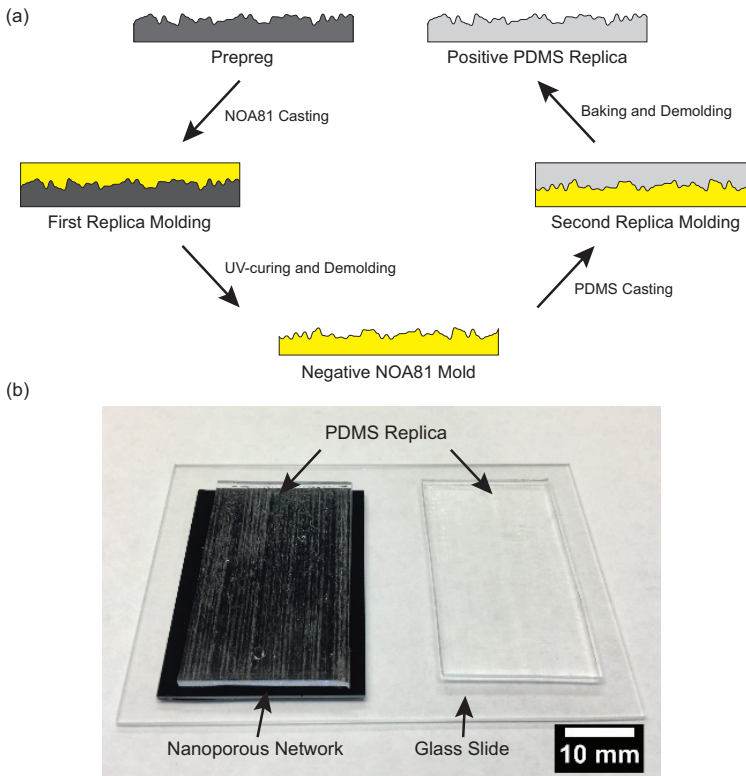


**FIGURE S4** Results of all manufacturing conditions: (a) short-beam strength, and (b) void content with standard error.

curing regardless of the existence of NPN. The reason why the OoO curing resulted in a lower void content than vacuum-only hot-plate curing is attributed to the existence of intralaminar voids, as presented in Figure S3b. The OoO curing showed the "sweep-like effect" to decrease intralaminar voids, which is discussed in the Supporting Information Section S7 and S8. Additionally, we observed that the order of manufacturing condition from the highest to the lowest value of short-beam strength matched that from the lowest to the highest value of void content. This observation also corroborates the findings from previous studies that high void content can cause detrimental effects on matrix-dominated properties and lifespan of composite parts such as interlaminar shear strength, flexural strength, and fatigue resistance [1–6].

## S5 | CONFORMABILITY OF NANOPOROUS NETWORK ON PREPREGS

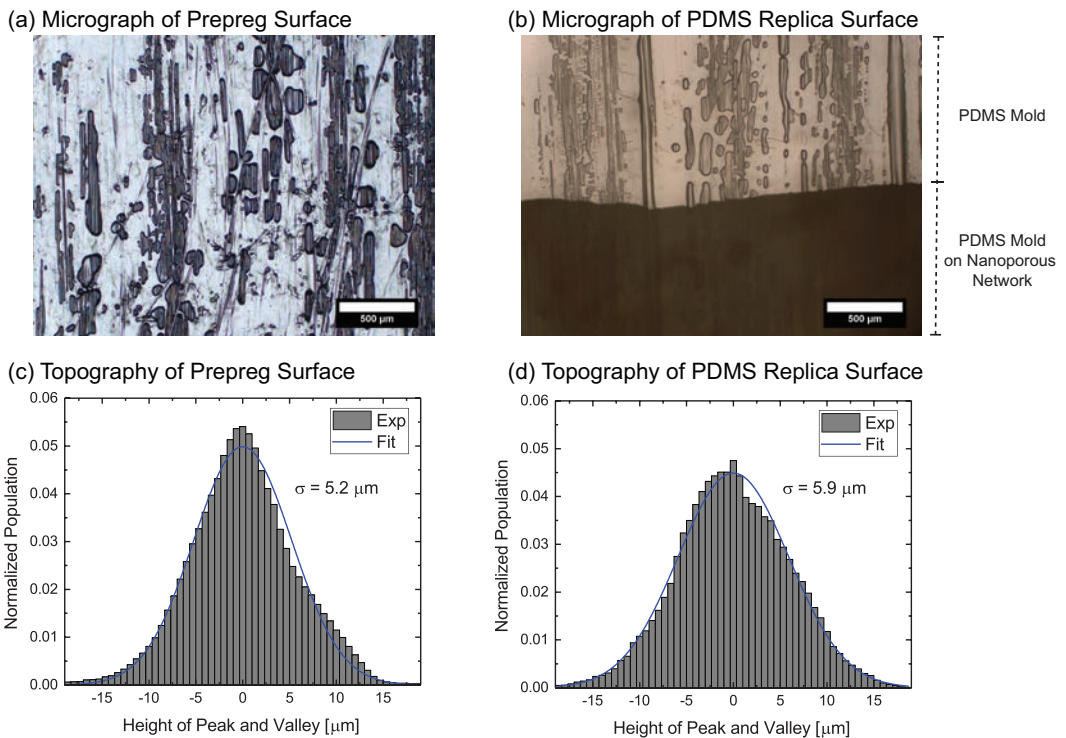
Since prepreg and NPN are not optically transparent, it is difficult to investigate the interfaces between them. Therefore, an optically transparent replica, that represents the surface profile of a prepreg, was created to observe the interfaces. First, a negative mold of the surface of a prepreg was fabricated with thiolene-based UV-curable resin NOA81 (Norland Products Inc., Cranbury, NJ, USA) because thermal rise during curing lowers the viscosity of the polymer in a prepreg and changes the morphology of the surface profile of the prepreg as well. For the negative mold, NOA81 was deposited on the surface of a prepreg to avoid air entrapment and cured under UV exposure of 365 nm, 9 W, and 2 min. Once UV-cured, the prepreg was rinsed with acetone and isopropyl alcohol and removed from the negative mold. For the second casting, Polydimethylsiloxane (PDMS) was used because of its ease of soft lithography and optical transparency [10, 11]. PDMS was mixed in a 10:1 ratio of PDMS monomer and curing agent (Sylgard 184 from Dow Corning, USA), and degassed by a planetary centrifugal mixer (Thinky mixer ARE-310). The PDMS mixture was poured onto the negative mold, and then cured in an oven at 70 °C for 6 hours. After curing, the PDMS layer was peeled off from the negative mold, and used as a replica of a prepreg. Figure S5 shows the fabrication process of a replica and images of the fabricated PDMS replica of the prepreg surface.



**FIGURE S5** PDMS replica for evaluation of NPN conformability to prepreg surface: (a) Schematic of the fabrication process of a PDMS replica of irregular surface of a prepreg, and (b) fabricated PDMS replica. Since a thermal process can change the morphology of the surface of a prepreg, the negative mold was fabricated using UV-curable resin, and then the positive replica made of PDMS was molded using a thermal process.

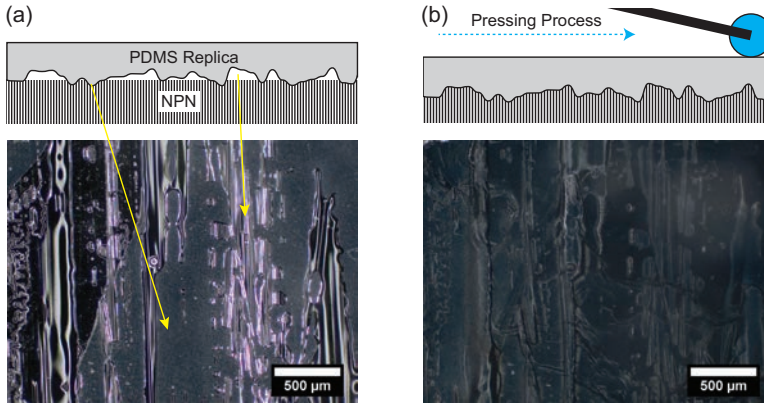
During manufacturing process of a prepreg, the reinforcements such as continuous carbon fibers are subjected to the impregnation process with polymers. The resulting prepreg may contain partially impregnated regions and an irregular surface finish. As presented in Figure S6a, there are some regions of exposed carbon fibers which are not covered with polymer, and such regions account for the irregular surface finish of a prepreg, resulting in air entrapment in the interlaminar regions during a lay-up process. Figure S6b presents a micrograph of the surface of a PDMS replica, and suggests that the morphology of micro-features are similar to that on a prepreg, as compared to Figure S6a. In order to compare quantitatively, the topography of the irregular surfaces of a prepreg and its PDMS replica were investigated by stylus profilometry with Dektak XT Stylus Profiler (Bruker, USA). An area of  $1.2\text{ cm} \times 1.2\text{ cm}$  was inspected with a  $2\text{ }\mu\text{m}$  radius stylus tip. As shown in Figure S6c and d, the height of micro-features on both prepreg and PDMS replica is normally distributed, and their standard deviations were  $5.2\text{ }\mu\text{m}$  and  $5.9\text{ }\mu\text{m}$ , respectively. Given that the measured area of  $1.2\text{ cm} \times 1.2\text{ cm}$  was randomly assigned in each sample, it is concluded that the PDMS replica is representative of the topography of the studied prepreg.

Figure S7 shows NPN conforming during the pressing process of laminate layup. Figure S7a is an illustration and dark-field image of the interface when a PDMS replica was placed on the NPN. As presented, the micro-features were partially contacted with NPN prior to the pressing procedure with a hand roller, which is a typical procedure for lamination. After the pressure was applied to the mold by a hand roller, NPN was compressed with varying degrees



**FIGURE S6** Comparison of prepreg and PDMS replica surfaces: optical micrograph of (a) prepreg surface and (b) PDMS replica surface; characterization of the topography of (c) prepreg surface and (d) PDMS replica. Note that the lower half of the PDMS mold is covered with NPN. The height of micro-features on both prepreg and PDMS replica shows a normal distribution.

depending on local spatial pressure, conforming to the profile of micro-features and resulting in full contact between the micro-features and NPN (see Figure S7b). Additional pressure for conforming is of course applied in the OoO with NPN manufacturing process from the applied vacuum pressure. Moreover, in order to evaluate whether both the top and bottom interfaces of NPN conform, the NPN (i.e., vertically aligned CNT arrays of  $\sim 20\ \mu\text{m}$  in height) were sandwiched between PDMS mold replicas of the prepreg surfaces, simulating a laminate lay-up. For both PDMS replicas at the top and bottom, the pressing procedure with a hand roller was applied to simulate a prepreg hand lay-up. We evaluated whether both the top and bottom interfaces of NPN conform, and the dark-field micrographs of each interface are presented in Figure S8. As can be seen, both interfaces were in full contact with NPN such that there was no bright regions in the dark-field micrographs after only the hand layup process.



**FIGURE S7** Illustration and representative dark-field image of the interface between a PDMS replica and NPN: (a) before, and (b) after the pressing procedure with a hand roller. Note that the dark-field image was taken from the same location.

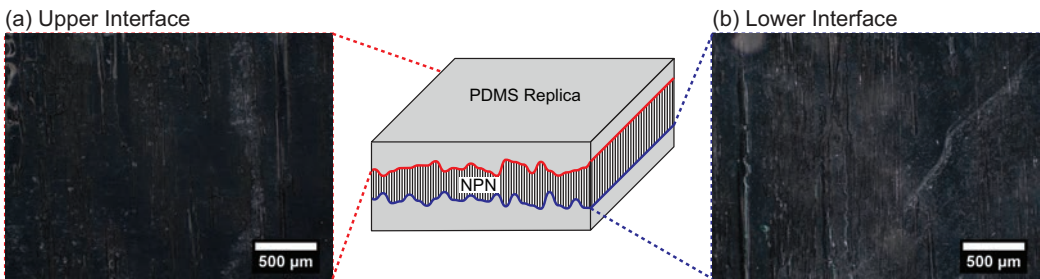


**FIGURE S8** Dark-field images of: (a) the interface between the upper PDMS replica and NPN, and (b) the interface between the lower PDMS replica and NPN after the pressing procedure with a hand roller during composite layup.

## S6 | NANO-ENGINEERED VACUUM CHANNEL FORMED BY NANOPOROUS NETWORK

Figure S9 shows representative X-ray micrographs of 16-ply quasi-isotropic laminate with and without NPN in the interlaminar region. It should be noted that these micrographs were taken prior to the curing process. As previously described in Figure 3, the baseline (i.e., a laminate without NPN) shows intrinsic void sources comprised of partially impregnated carbon fiber tows in the intralaminar regions, and entrapped air pockets in the interlaminar regions. Most importantly, the interlaminar void clusters in a lamina were not likely to be connected to either those of adjacent laminae or in the same lamina, and the interlaminar voids formed macro air pockets. In other words, these voids were not likely to be connected to each other through either in-plane or transverse routes. However, as presented in Figure S9b, the laminate with CNT arrays showed a distinct horizontally aligned channel at each interlaminar region, due to the vertically-aligned CNT NPN. Unlike the baseline specimens without NPN, here voids at the interlaminar regions formed connected air pockets, and rather connected toward the laminate edges *via* the NPN, forming channel-like architectures. In addition, the intralaminar voids in a lamina can be connected to those of adjacent laminae through such architectures. Since the CNT array is a NPN having a low volume fraction of <5% [12, 13], it is imaged as voids due to the low attenuation of X-ray, and also has a high gas permeability [14, 15]. The observation implies that the NPN may increase the in-plane and transverse gas permeability of a laminate through the highly permeable CNT arrays at the interlaminar regions, leading to the effective evacuation of voids within a laminate during the epoxy flow and curing processes. This approach is similar to the principle mechanism of OoA preregs. One OoA prepreg mechanism achieves the removal of entrapped air by partially impregnated microstructures consisting of both dry pathways (i.e., engineered vacuum channels or EVaCs) and resin-rich area, which form a permeable vascular network that allows gas migration towards the laminate boundaries [16–18]. Prior OoA studies reported that the higher gas permeability

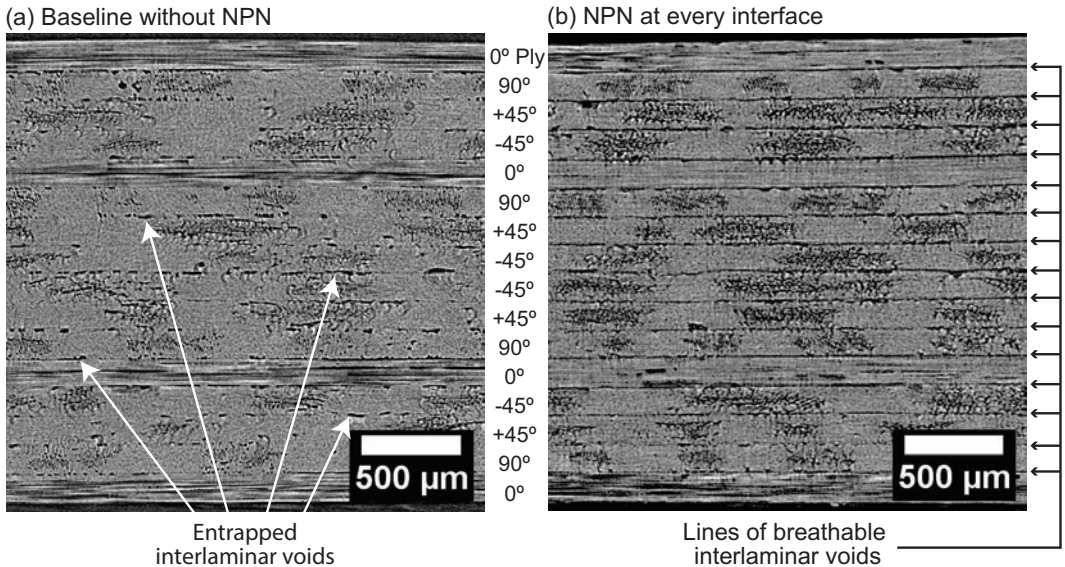


**FIGURE S9** Representative X-ray micrographs of an *uncured* 16-ply quasi-isotropic autoclave prepreg laminate: (a) without NPN, and (b) with NPN. Voids were connected together either directly or indirectly in the NPN case, forming channel-like architectures at the interlaminar regions.

of OoA prepreps during impregnation results in much less time to evacuate the gases from a laminate [19]. Future work should explore the gas permeability measurement of laminates with NPN to gain additional understanding of gas transport during curing.

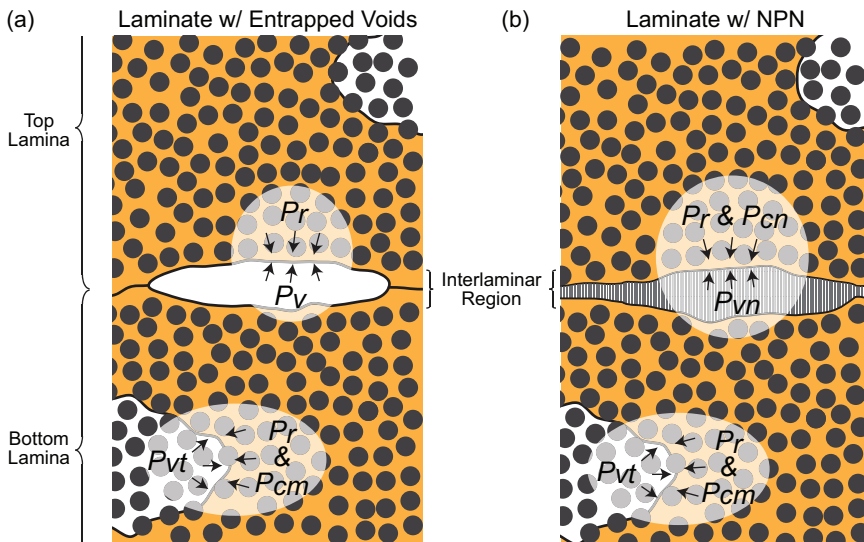
## S7 | VOID EXTRACTION IN INTRALAMINAR REGION

Figure S10 presents the cross-section of an uncured laminate with and without conformable NPN, showing the pressure boundary condition in both the interlaminar and intralaminar regions. There are intrinsic void sources in a laminate, comprised of unimpregnated dry tows in the intralaminar region, and entrapped air during the prepreg lay-up procedure located in the interlaminar region. In the case of the intralaminar region, the resin pressure ( $P_r$ ) and gas pressure within the dry tow ( $P_{vt}$ ), and capillary pressure to the micro-scale fiber tows ( $P_{cm}$ ) are applied at the resin flow front; the pressure gradient toward the dry tows corresponds to  $\Delta P = P_r + P_{cm} - P_{vt}$ . When only vacuum is applied during curing,  $P_r$  can be taken as  $\leq 0.1$  MPa. Since most of the dry tows can be subjected to a vacuum due to a higher permeability along the fibers,  $P_{vt}$  is assumed to be  $\sim 0$  MPa.  $P_{cm}$  can be estimated with morphological characteristics of the dry tows and the assumption of one-dimensional resin flow perpendicular to the fiber alignment [20–22] as follows:

$$P_{cm} = \frac{2}{D_f} \frac{1 - \varepsilon}{\varepsilon} \sigma \cos \theta \quad (S1)$$

Note that a prefactor of 2 instead of 4 is used in this equation, because the resin flow is perpendicular to the fiber alignment.  $D_f = 7.1 \mu\text{m}$  and  $\varepsilon = 0.4$  are obtained from the prepreg data sheet from manufacturer, and  $\sigma \approx 35 \text{ mJ m}^{-1}$  and  $\theta \approx 20^\circ$  are reasonable to be assumed as a thermoset resin [23–25]. Thus,  $P_{cm}$  of 0.014 MPa is estimated, corresponding to  $\Delta P \sim 0.114$  MPa. Therefore, the resin wetting toward the dry tows is anticipated, and the intralaminar region of a laminate with NPN is expected to be in the same situation, i.e., unchanged by the presence of the NPN in the interlaminar region.

In the case where the intralaminar voids are relatively hard to be removed by a vacuum (e.g., cm-scale laminates),



**FIGURE S10** Illustration of the pressure boundary condition in a laminate with: (a) entrapped air due to the irregular surface of prepreg layers, and (b) conformable NPN (i.e., vertically aligned carbon nanotube arrays) in the interlaminar region.

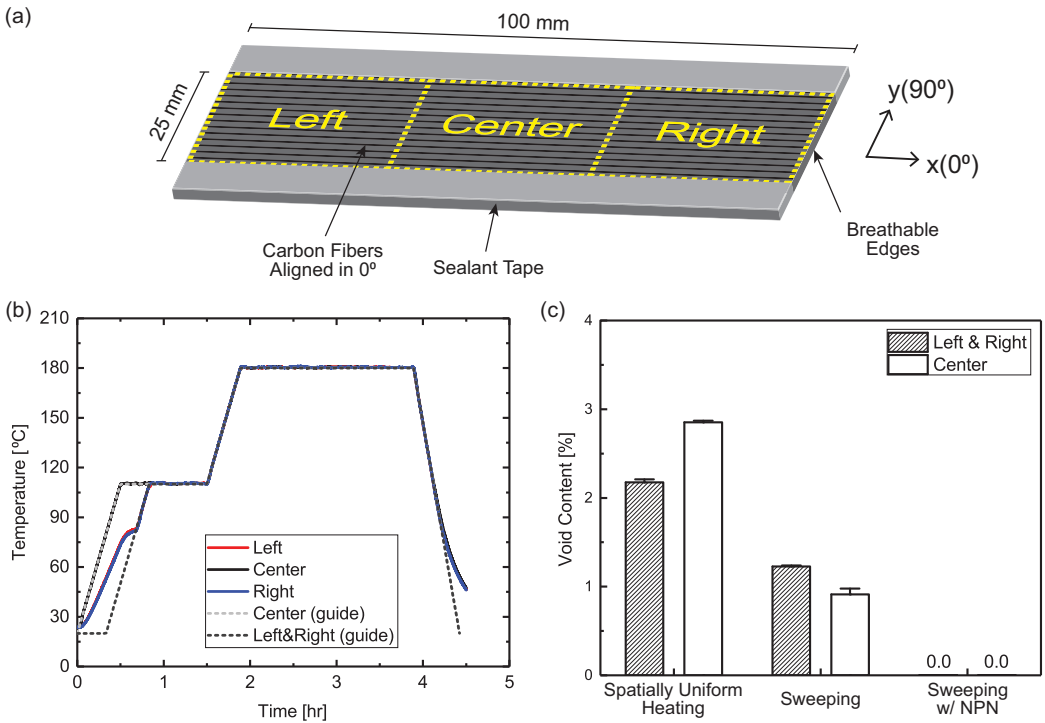
we found that the sweep-like effect by zonal heating via OoO curing helps to reduce the intralaminar voids (see the Supporting Information Section S8). Polymer impregnation into dry tows may occur at random locations during a cure cycle. Such random impregnation of the polymer into the dry tows may block the void evacuation network and hinder effective void migration outward at the edges. By an asynchronous zonal heating with multiple heaters for OoO curing, we found that the voids at the center were removed first through the breathable void networks at the sides, and then the voids at the sides were evacuated easily with a relatively short migration distance to the edges of the laminate. Given these results, it is demonstrated that the laminates comprised of autoclave prepregs can be successfully cured only under a vacuum via the NPN, and may be effectively supplemented with the void sweeping method. Furthermore, the concept of void sweeping can be readily combined with conventional composite curing processes such as autoclave and oven curing because OoO curing is based on a vacuum-bag-only curing. Therefore, we expect that this technique will be useful for manufacturing complex composite structures (e.g., high curvature, tapers in ply and in-plane geometry), which usually contain relatively high void content [26].

## S8 | INTRALAMINAR VOID SWEEPING BY ZONAL HEATING VIA OOO CURING

During a cure cycle, the viscosity of the polymer initially decreases as the temperature ramps up. Then, the viscosity quickly increases towards a solid as the gelation occurs and cross-linking of the polymer proceeds. Once gelation occurs, void migration is effectively restricted due to the limited movement of the polymer chains. Therefore, it is important to have a practical time period with a relevant viscosity value range so that effective void evacuation is possible [27, 28]. Moreover, in the situation where an applied pressure is not applied (e.g., OoA curing), it is known that breathable laminate edges are required in some systems for a low void content [17, 29–31]. Previous studies suggest that the connected and open void network within a laminate during void evacuation is a key feature for acquiring low void content.

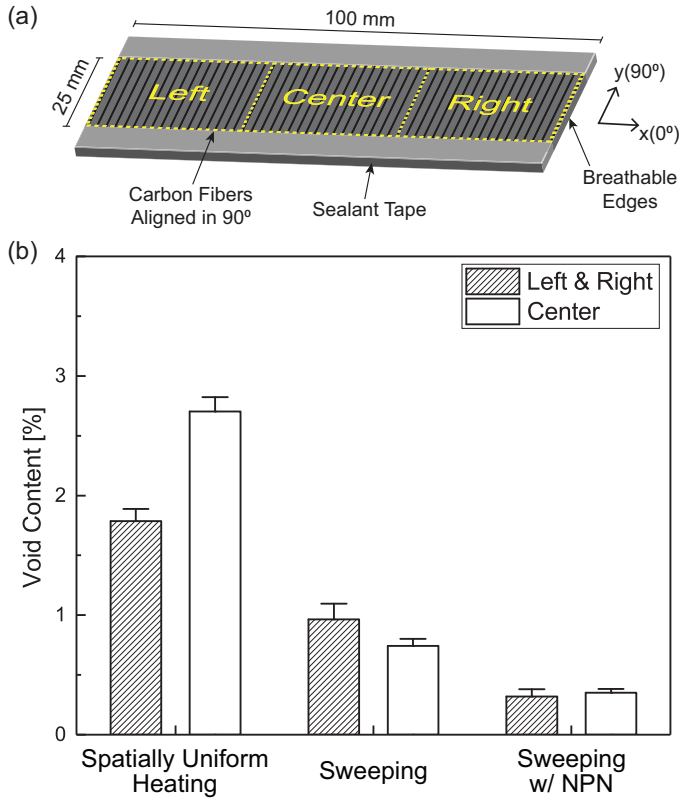
During the preliminary analysis of the void content under different manufacturing conditions, it was observed that the laminate edges experienced lower temperature than the inner regions during the OoO curing, due to edge effects and likely insufficient thermal insulation. Thus, it was hypothesized that such temperature gradients might help maintain the connected and open void network during a cure cycle, which gives rise to the lower observed void content in the OoO specimens (see Section S4). If the heating during the void evacuation period is spatially uniform, polymer impregnation into dry regions may occur at random locations. Such random impregnation of the polymer into the dry regions may block the void evacuation network and hinder effective void migration outward at the edges. However, if the temperature at the center of a laminate is higher than that at the edges, the impregnation tends to proceed from the center to the edges, keeping the void network connected to a vacuum. As a result, voids within a laminate are removed effectively with a spatial sweep-like effect. To investigate this, we carried out an OoO curing with an intentional in-plane temperature gradient by asynchronous heating with multiple heaters. A 100 mm × 25 mm 16-ply unidirectional laminate (Hexcel Hexply AS4/8552 autoclave-formulated prepreg) was used, and the fibers were aligned with the long sides. To restrict the direction of void evacuation along the fiber alignment direction, the long edges of the laminate were sealed with a vacuum sealant tape. Three electrically isolated CNT film heaters were installed on the left, center, and right region of the laminate (see Figure S11a). In order to create void sweeping, a time delay of 20 min was applied (see "guide" lines in Figure S11b) to the heaters installed at the side regions during the first temperature ramp up, while the heater at the center followed the cure cycle provided from the manufacturer. Once the temperature of each heater reached the first hold point of 120 °C, all heaters were synchronized to minimize the thermally induced residual stress (see Figure S11b). Note that the right and left regions were heated in the first ramp-up due to the center region heating and thermal conduction, even though they were only powered after the 20 minute delay.

Figure S11c presents the void content at the center and sides under the spatially uniform heating vs. sweeping conditions. Since we found that a nanoporous network (NPN) helps to lower the void content, the sweeping experiment was additionally conducted on a laminate with NPN. As expected, the spatially uniform heating showed void content of ~1.8% and ~3.1% at the sides and center of the laminate, respectively. The results indicate that the void evacuation can be hindered by the blockage of void networks. The center part has higher potential to be disconnected to a vacuum than the sides, which results in the higher void content at the center. However, the sweeping condition exhibited the opposite results. The void content at the center was ~0.3%, which is lower than that at the sides of ~1.0%. Both at the center and sides, the void content after sweeping were lower than those under spatially uniform heating. These results indicate that the voids at the center were removed first through the intact breathable void networks at the sides, and then the voids at the sides were evacuated easily with a relatively short migration distance to the edges of the laminate. Most importantly, when sweeping was combined with NPN, there was no detectable void



**FIGURE S11** Effects of void sweeping on final void content for a 0° unidirectional laminate: (a) Illustration of a 0° unidirectional laminate subjected to the void sweeping experiment, (b) temperature profiles during the void sweeping, and (c) void content at the center and sides of the laminate cured by spatially uniform heating and sweeping, with and without NPN. Three independent heaters at the left, center, and right region were controlled to perform the void sweeping. Note that the long edges of the laminate were sealed with a vacuum sealant tape so that only the short edges at the left and right regions were breathable. The "guide" temperature profiles indicate the hypothetical guideline temperatures for sweeping. Due to the in-plane heat conduction from the center part, the side regions heated up despite of an intentional time delay for sweeping. The whiskers represent standard error.

throughout the laminate. In addition to this void sweeping along the micro fiber alignment direction, experiments in the transverse direction were performed as the worst case scenario (see Figure S12a). This is because the morphology of the void network is elongated along the fiber alignment direction, and also voids are more likely to be evacuated along the microfibers than transversely [19, 32]. Thus, the final void content from experiments in the transverse direction (90° laminate, as in Figure S12) exhibited relatively higher void content than that along the fiber (0° laminate, as in Figure S11), yet showed the same trends overall. Given these results, we conclude that the laminates comprised of autoclave prepreps can be successfully cured under only a vacuum *via* the NPN, and may be effectively supplemented with the void sweeping method at larger scales or when structural complexity increases beyond flat plates. Furthermore, the concept of void sweeping can be readily combined with conventional composite curing processes such as autoclave and oven curing because OoO curing is based on a vacuum-bag-only curing. Therefore, we expect that this technique will be useful for manufacturing complex composite structures, which usually contain relatively high void content, vs. basic structures like plates [26]. These results on void sweeping are considered preliminary and need significant follow-up work.

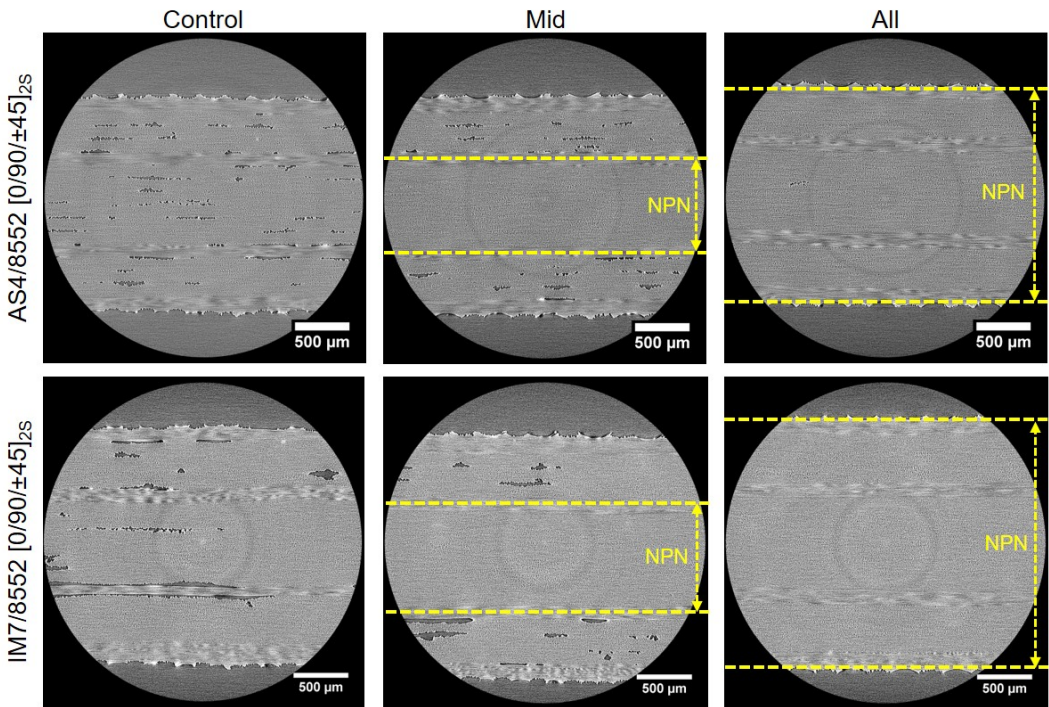


**FIGURE S12** Effects of void sweeping on void content for a 90° laminate. (a) Illustration of an 90° unidirectional laminate subjected to the void sweeping experiment, and (b) the results of void content at the center and sides of the laminate. Note that three independent heaters at the left, center, and right regions were controlled to conduct the void sweeping. The long edges of the laminate were sealed with a vacuum sealant tape so that only the short edges at the left and right regions were breathable. The whiskers represent standard error.

## S9 | ALTERNATIVE COMPOSITE AND EFFECT OF NPN PLACEMENT

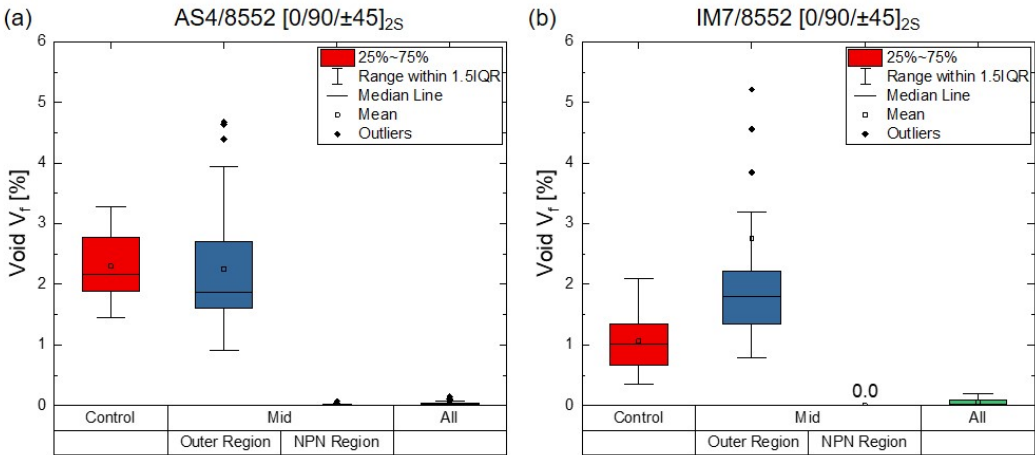
Three configurations were tested to evaluate the effect of NPN placement on an additional composite prepreg (i.e., Hexcel IM7/8552) as follows: a laminate without NPN ("Control"); a laminate with NPNs at 7 interlaminar regions in the middle ("Mid"); a laminate with NPNs at all 15 interlaminar regions ("All"). Both prepreg systems (i.e., Hexcel AS4/8552 and IM7/8552 aerospace-grade unidirectional carbon fiber prepreps) were directly compared. It should be noted that these prepreps are designed to be processed with applied pressure using an autoclave. For the laminates, 16 plies of 3 cm × 3 cm were used in the quasi-isotropic layup of  $[0/90/\pm 45]_{2S}$ , and the NPNs were installed in the designated interlaminar regions during hand-layup process. The laminates were cured at the same time using a hot plate (i.e., EchoTherm HS60A) so that batch-to-batch thermal variations were minimized. After the hand lay-up process of the laminates, vacuum debulking was performed on the full laminates at room temperature for 3 hours. During the cure cycle, the recommended cure cycle in the technical data sheet was followed [33], and the vacuum bag was kept under full vacuum (i.e., >29.5 inHg) during the entire process.  $\mu$ CT imaging of laminates was performed with ZEISS Xradia 520 Versa at the Institute for Soldier Nanotechnologies, MIT. An isotropic voxel size of 1.5  $\mu$ m was used with an X-ray beam energy of 7 W at 80 kV. For each scan, 3201 2D-projections were acquired while a specimen was rotated 360°. The exposure time for each projection was 1 second, and the projection radiographs were reconstructed using the embedded software in the CT machine.

Figure S13 shows representative  $\mu$ CT slices of AS4/8552 and IM7/8552 laminates in three NPN placement cases



**FIGURE S13**  $\mu$ CT slices of AS4/8552 and IM7/8552 in three NPN placement cases: Control, Mid, and All. In both prepreg systems, NPNs significantly reduced the voids in the interlaminar regions where they were installed.

(i.e., “Control”, “Mid”, and “All”). The areas where NPNs were installed are indicated in Figure S13. In X-ray micrographs, the brighter gray-scaled regions denote denser areas such as fibers and polymers, while the voids appear as darker. The quantified void contents from 40 slices for each case are presented in Figure S14. Of note, in the case of the “Mid” specimen, void contents were quantified in two separate regions depending on the existence of NPN. The “Control” specimens cured without applied pressure showed a void fraction of ~2.4% and ~1.0% in AS4/8552 and IM7/8552, respectively. This is because vacuum alone is not sufficient to remove voids or to suppress the void formation within a laminate. However, when NPNs were installed in the interlaminar regions on the middle of the laminates (see the “Mid” case), the void contents of AS4/8552 and IM7/8552 were effectively reduced in the middle part where NPNs were introduced. Moreover, there was no detectable void in the middle part of the IM7/8552 laminate. On the contrary, the outer regions without NPNs showed a high void content (> 1%) as much as the “Control” specimens did. In the case of “All”, the AS4/8552 and IM7/8552 laminates showed very low void content (< 0.1%), which is comparable with the quality of autoclave-cured laminate. The results concluded that NPNs significantly reduced the voids in the regions where they were installed. Therefore, in order to manufacture a void-free laminate, NPNs need to be installed in all interlaminar regions. In addition, given that the NPN showed similar results in two different prepreg systems, it can be concluded that the effect of NPN is somewhat generalizable.

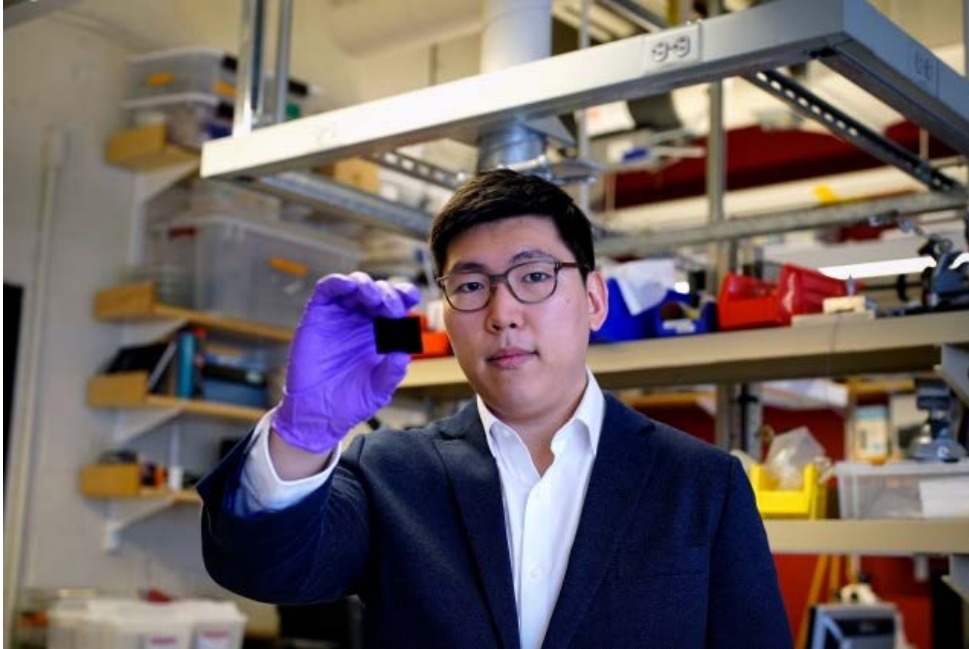


**FIGURE S14** Void content of (a) AS4/8552 and (b) IM7/8552 composite laminates cured under a vacuum without NPN (Control), with NPNs only in the middle half of the laminate (Mid), and with NPNs in all interlaminar regions (All).

## references

- [1] PBAUPS Olivier, J P Cottu, and BBAUPS Ferret. Effects of cure cycle pressure and voids on some mechanical properties of carbon/epoxy laminates. *Composites*, 26(7):509–515, 1995.
- [2] S R Ghiorse. Effect of void content on the mechanical properties of carbon/epoxy laminates. *SAMPE quarterly*, 24(2):54–59, 1993.
- [3] Hongyan Zhu, Baochang Wu, Dihong Li, Dongxing Zhang, and Yuyong Chen. Influence of voids on the tensile performance of carbon/epoxy fabric laminates. *Journal of Materials Science & Technology*, 27(1):69–73, 2011.
- [4] Ling Liu, Bo-Ming Zhang, Dian-Fu Wang, and Zhan-Jun Wu. Effects of cure cycles on void content and mechanical properties of composite structures. *Composite Structures*, 73(3):303–309, 2006.
- [5] A R Chambers, J S Earl, C A Squires, and M A Suhot. The effect of voids on the flexural fatigue performance of unidirectional carbon fibre composites developed for wind turbine applications. *International Journal of Fatigue*, 28(10):1389–1398, 2006.
- [6] Nigel C W Judd and W W Wright. Voids and their effects on the mechanical properties of composites- an appraisal. *Sampe Journal*, 14:10–14, 1978.
- [7] Jeonyoon Lee. *In situ curing of polymeric composites via resistive heaters comprised of aligned carbon nanotube networks*. PhD thesis, Massachusetts Institute of Technology, 2014.
- [8] Jeonyoon Lee, Itai Y. Stein, Seth S. Kessler, and Brian L. Wardle. Aligned carbon nanotube film enables thermally induced state transformations in layered polymeric materials. *ACS Applied Materials and Interfaces*, 7(16):8900–8905, apr 2015.
- [9] Jeonyoon Lee, Xinchun Ni, Frederick Daso, Xianghui Xiao, Dale King, Jose Sánchez Gómez, Tamara Blanco Varela, Seth S. Kessler, and Brian L. Wardle. Advanced carbon fiber composite out-of-autoclave laminate manufacture via nanostructured out-of-oven conductive curing. *Composites Science and Technology*, 2018.
- [10] Leonid Gitlin, Philipp Schulze, and Detlev Belder. Rapid replication of master structures by double casting with PDMS. *Lab on a Chip*, 9(20):3000–3002, 2009.
- [11] Michael W Toepke and David J Beebe. PDMS absorption of small molecules and consequences in microfluidic applications. *Lab on a Chip*, 6(12):1484–1486, 2006.
- [12] Jeonyoon Lee, Itai Y Stein, Mackenzie E Devoe, Diana J Lewis, Noa Lachman, Samuel T Buschhorn, Seth S Kessler, and Brian L Wardle. Impact of carbon nanotube length on electron transport in aligned carbon nanotube networks The MIT Faculty has made this article openly available . Please share Citation and Brian L . Wardle . “ Impact of Carbon Nanotube Length on Publisher Version Access. *Applied Physics Letters*, 106(5):–, 2015.
- [13] Itai Y Stein and Brian L Wardle. Coordination number model to quantify packing morphology of aligned nanowire arrays. *Physical chemistry chemical physics : PCCP*, 15(11):4033–40, 2013.
- [14] Bruce J Hinds, Nitin Chopra, Terry Rantell, Rodney Andrews, Vasilis Gavalas, and Leonidas G Bachas. Aligned Multiwalled Carbon Nanotube Membranes. *Science*, 303(5654):62 LP – 65, jan 2004.
- [15] Jason K Holt, Hyung Gyu Park, Yinmin Wang, Michael Stadermann, Alexander B Artyukhin, Costas P Grigoropoulos, Aleksandr Noy, and Olgica Bakajin. Fast Mass Transport Through Sub-2-Nanometer Carbon Nanotubes. *Science*, 312(5776):1034 LP – 1037, may 2006.
- [16] Leyla Farhang. *Void evolution during processing of out-of-autoclave prepreg laminates*. PhD thesis, University of British Columbia, 2014.
- [17] Melanie Brilliant. Out-of-Autoclave Manufacturing of Complex Shape Composite Laminates. *Mechanical Engineering*, (December), 2010.

- [18] Thomas a Cender, John J Gangloff Jr, Pavel Simacek, and Suresh G Advani. Void Reduction During Out-of-Autoclave Thermoset Prepreg Composite Processing. In *SAMPE 2014 Proceedings*, number JUNE, 2014.
- [19] Ara Arafath. Gas transport in prepregs: model and permeability experiments. In *Proceedings of the ICCM -17*, number October 2015, 2009.
- [20] K. J. Ahn, J. C. Seferis, and J. C. Berg. Simultaneous measurements of permeability and capillary pressure of thermosetting matrices in woven fabric reinforcements. *Polymer Composites*, 12(3):146–152, 1991.
- [21] M. T. Senoguz, F. D. Dungan, A. M. Sastry, and J. T. Klamo. Simulations and experiments on low-pressure permeation of fabrics: Part II - The variable gap model and prediction of permeability. *Journal of Composite Materials*, 35(14):1285–1322, 2001.
- [22] C. Lekakou and M.G. Bader. Mathematical modelling of macro- and micro-infiltration in resin transfer moulding (RTM). *Composites Part A: Applied Science and Manufacturing*, 29(1-2):29–37, 1998.
- [23] Stéphane A Page, Raffaele Mezzenga, Louis Boogh, John C Berg, and Jan-Anders E Månson. Surface Energetics Evolution during Processing of Epoxy Resins. *Journal of Colloid and Interface Science*, 222(1):55–62, 2000.
- [24] K Grundke, P Uhlmann, T Gietzelt, B Redlich, and H.-J. Jacobasch. Studies on the wetting behaviour of polymer melts on solid surfaces using the Wilhelmy balance method. *Colloids and Surfaces A: Physicochemical and Engineering Aspects*, 116(1):93–104, 1996.
- [25] M Hautier, D Lévêque, C Huchette, and P Olivier. Investigation of composite repair method by liquid resin infiltration. *Plastics, Rubber and Composites*, 39(3-5):200–207, jun 2010.
- [26] Y. Ma, T. Centea, G. Nilakantan, and S. Nutt. Vacuum bag only processing of complex shapes: Effect of corner angle, material properties and processing condition. In *American Society for Composites - 29th Technical Conference, ASC 2014; 16th US-Japan Conference on Composite Materials; ASTM-D30 Meeting*, 2014.
- [27] F Y C Boey and S W Lye. Void reduction in autoclave processing of thermoset composites: Part 1: High pressure effects on void reduction. *Composites*, 23(4):261–265, 1992.
- [28] F Y C Boey and S W Lye. Void reduction in autoclave processing of thermoset composites: Part 2: Void reduction in a microwave curing process. *Composites*, 23(4):266–270, 1992.
- [29] L Repecka and J Boyd. Vacuum-bag-only-curable prepregs that produce void-free parts. In *Proceedings of the SAMPE 2002 Conference*, pages 1862–1874, 2002.
- [30] Chris Ridgard. Out of autoclave composite technology for aerospace, defense and space structures. In *Proceedings of the SAMPE 2009 Conference*, 2009.
- [31] Gary G Bond, J M Griffith, G L Hahn, C Bongiovanni, and J Boyd. A study of non-autoclave prepreg manufacturing technology. *SAMPE journal*, 45(3):6–19, 2009.
- [32] Thomas A Cender, Pavel Simacek, Steven Davis, and Suresh G Advani. Gas Evacuation from Partially Saturated Woven Fiber Laminates. *Transport in Porous Media*, 115(3):541–562, dec 2016.
- [33] Hexcel. HexPly 8552 product data sheet.



MIT postdoc Jeonyoon Lee

Image: Melanie Gonick, MIT

## A new approach to making airplane parts, minus the massive infrastructure

Carbon nanotube film produces aerospace-grade composites with no need for huge ovens or autoclaves.

**Jennifer Chu | MIT News Office**  
**January 13, 2020**

A modern airplane's fuselage is made from multiple sheets of different composite materials, like so many layers in a phyllo-dough pastry. Once these layers are stacked and molded into the shape of a fuselage, the structures are wheeled into warehouse-sized ovens and autoclaves, where the layers fuse together to form a resilient, aerodynamic shell.

Now MIT engineers have developed a method to produce aerospace-grade composites without the enormous ovens and pressure vessels. The technique may help to speed up the manufacturing of airplanes and other large, high-performance composite structures, such as blades for wind turbines.

The researchers detail their new method in a paper published today in the journal *Advanced Materials Interfaces*.

"If you're making a primary structure like a fuselage or wing, you need to build a pressure vessel, or autoclave, the size of a two- or three-story building, which itself requires time and money to pressurize," says Brian Wardle, professor of aeronautics and astronautics at MIT. "These things are massive pieces of infrastructure. Now we can make primary structure materials without autoclave pressure, so we can get rid of all that infrastructure."

### RELATED

Brian Wardle

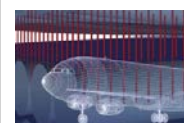
Department of Aeronautics and Astronautics

School of Engineering

### ARCHIVES



Pantry ingredients can help grow carbon nanotubes



Carbon nanotube "stitches" strengthen composites

Taking aircraft

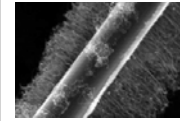
Wardle's co-authors on the paper are lead author and MIT postdoc Jeonyoon Lee, and Seth Kessler of Metis Design Corporation, an aerospace structural health monitoring company based in Boston.



manufacturing out of the oven

### Out of the oven, into a blanket

In 2015, Lee led the team, along with another member of Wardle's lab, in creating a method to make aerospace-grade composites without requiring an oven to fuse the materials together. Instead of placing layers of material inside an oven to cure, the researchers essentially wrapped them in an ultrathin film of carbon nanotubes (CNTs). When they applied an electric current to the film, the CNTs, like a nanoscale electric blanket, quickly generated heat, causing the materials within to cure and fuse together.



Planes, trains and automobiles: faster, stronger, lighter

With this out-of-oven, or OoO, technique, the team was able to produce composites as strong as the materials made in conventional airplane manufacturing ovens, using only 1 percent of the energy.

The researchers next looked for ways to make high-performance composites without the use of large, high-pressure autoclaves — building-sized vessels that generate high enough pressures to press materials together, squeezing out any voids, or air pockets, at their interface.

“There's microscopic surface roughness on each ply of a material, and when you put two plies together, air gets trapped between the rough areas, which is the primary source of voids and weakness in a composite,” Wardle says. “An autoclave can push those voids to the edges and get rid of them.”

Researchers including Wardle's group have explored “out-of-autoclave,” or OoA, techniques to manufacture composites without using the huge machines. But most of these techniques have produced composites where nearly 1 percent of the material contains voids, which can compromise a material's strength and lifetime. In comparison, aerospace-grade composites made in autoclaves are of such high quality that any voids they contain are negligible and not easily measured.

“The problem with these OoA approaches is also that the materials have been specially formulated, and none are qualified for primary structures such as wings and fuselages,” Wardle says. “They're making some inroads in secondary structures, such as flaps and doors, but they still get voids.”

### Straw pressure

Part of Wardle's work focuses on developing nanoporous networks — ultrathin films made from aligned, microscopic material such as carbon nanotubes, that can be engineered with exceptional properties, including color, strength, and electrical capacity. The researchers wondered whether these nanoporous films could be used in place of giant autoclaves to squeeze out voids between two material layers, as unlikely as that may seem.

A thin film of carbon nanotubes is somewhat like a dense forest of trees, and the spaces between the trees can function like thin nanoscale tubes, or capillaries. A capillary such as a straw can generate pressure based on its geometry and its surface energy, or the material's ability to attract liquids or other materials.

The researchers proposed that if a thin film of carbon nanotubes were sandwiched between two materials, then, as the materials were heated and softened, the capillaries between the carbon nanotubes should have a surface energy and geometry such that they would draw the materials in toward each other, rather than leaving a void between them. Lee calculated that the capillary pressure should be larger than the pressure applied by the autoclaves.

The researchers tested their idea in the lab by growing films of vertically aligned carbon nanotubes using a technique they previously developed, then laying the films between layers of materials that are typically used in the autoclave-based manufacturing of primary aircraft structures. They wrapped the layers in a second film of carbon nanotubes, which they applied an electric current to to heat it up. They observed that as the materials heated and softened in response, they were pulled into the capillaries of the intermediate CNT film.

The resulting composite lacked voids, similar to aerospace-grade composites that are produced in an autoclave. The researchers subjected the composites to strength tests, attempting to push the layers apart, the idea being that voids, if present, would allow the layers to separate more easily.

“In these tests, we found that our out-of-autoclave composite was just as strong as the gold-standard autoclave process composite used for primary aerospace structures,” Wardle says.

The team will next look for ways to scale up the pressure-generating CNT film. In their experiments, they worked with samples measuring several centimeters wide — large enough to demonstrate that nanoporous networks can pressurize materials and prevent voids from forming. To make this process viable for manufacturing entire wings and fuselages, researchers will have to find ways to manufacture CNT and other nanoporous films at a much larger scale.

“There are ways to make really large blankets of this stuff, and there’s continuous production of sheets, yarns, and rolls of material that can be incorporated in the process,” Wardle says.

He plans also to explore different formulations of nanoporous films, engineering capillaries of varying surface energies and geometries, to be able to pressurize and bond other high-performance materials.

“Now we have this new material solution that can provide on-demand pressure where you need it,” Wardle says. “Beyond airplanes, most of the composite production in the world is composite pipes, for water, gas, oil, all the things that go in and out of our lives. This could make making all those things, without the oven and autoclave infrastructure.”

This research was supported, in part, by Airbus, ANSYS, Embraer, Lockheed Martin, Saab AB, Saertex, and Teijin Carbon America through MIT’s Nano-Engineered Composite aerospace Structures (NECST) Consortium.

---

Topics: **Aeronautical and astronautical engineering**   **Carbon nanotubes**  
**Manufacturing**   **Materials Science and Engineering**   **Research**  
**School of Engineering**   **Nanoscience and nanotechnology**

---

## About This Website

This Website is maintained by the MIT News Office, part of the Office of Communications.

MIT News Office • Building 11-400  
Massachusetts Institute of Technology • Cambridge, MA 02139-4307